INTERNATIONAL ATOMIC ENERGY AGENCY
UNITED NATIONS EDUCATIONAL, SCIENTIFIC AND CULTURAL ORGANIZATION
INTERNATIONAL CENTRE FOR THEORETICAL PHYSICS
I.C.T.P., P.O. BOX 586, 34100 TRIESTE, ITALY, CABLE: CENTRATOM TRIESTE

SMR.705 - 27

COLLEGE ON SOIL PHYSICS

(6 - 24 September 1993)

"Soil Hydrology"

M. Kutilek
Czech Technical University
Katedra Hydromelioraci
Fakulta Stavebni
Thakurova 7
166 29 Prague
Czech Republic

MIREK KUTÍLEK

LECTURE NOTES
(COLLEGE ON SOIL PHYSICS)
ICTP

EX: "SOIL HYDROLOGY"
BY
M. KUTÍLEK & DON R. NIELSEN
(TO BE PUBLISHED IN 1994
BY CATENA)

1 SOILS IN HYDROLOGY

Soil is a very thin layer of the earth when its thickness is compared to the dimensions of the atmosphere or geosphere. Even the average depth of water in the oceans is orders of magnitude greater than that of soil. In spite of its slim dimension, soil is indispensable for life on continents. Without soil, our planet would not be green and all life would be restricted to the oceans.

Hydrologically, soil is an important reservoir of fresh water. Owing to the action of this reservoir, non continuous rainfall or snow are transformed into a continuous flow of water to the roots of plants. Together with ground waters, soil transforms discontinuous precipitation into continuous discharges recognized as streams and rivers. Without soil, the face of our planet would have continents wrinkled by dry wadis conducting water only during and immediately after each rainfall event. The retention capacity of soil able to sequester rain water is approximately the same as the capacity of all lakes. Moreover, the amount of water in soil equals one-third of all fresh water in lakes (including artificial reservoirs) and is one order of magnitude larger than that in riverbeds. On the other hand, the volume of ground waters is substantially greater than that in soil. Soil water together with ground water exceeds by more than two orders of magnitude all surface fresh water (Dyck and Peschke, 1983). Transport of water soluble materials occurring naturally or anthropogenically is linked to hydrologic processes. For example, without water as a transporting agent, anthropogenically derived chemical pollutants would remain at the location of their deposition provided they were not carried into the atmosphere by diffusion or the wind. The distance and rate of their motion on and below the soil surface depends upon hydrologic events. Because soil is a chemically and biologically active medium, pollutants are partly retained, released and transformed with the boundary of the pollution transposed in both time and space. Similarly, naturally occurring constituents within soil are mobilized and transported as a result of precipitation and irrigation. The quality of continental water resources in space and time is therefore greatly influenced by soil hydrology.

1.1 SOILS

INCEPTISOLS (*-ept*) Soils with a diagnostic cambic horizon having no aridic hydric regime. They correspond to Cambisols (FAO) with some Great Groups equivalent to some Soil Units of Luvisols (FAO), e. g. Ustochrepts being equivalent to Calcic Luvisols.

MOLLISOLS (*-oll*) Soils with a deep mollic humus horizon. Borolls with a frigid temperature regime and Ustolls with an ustic (nearly dry) moisture regime correspond to Chernozems (FAO) while Udolls with a udic (humid) moisture regime are equivalent to Phaeozems (FAO). Argiudolls and Argiborolls with an argillic (clay) horizon correspond to Greyzems (FAO).

OXISOLS (*-ox*) Soils with an oxic horizon characterized by kaolinites in the clay fraction and few weatherable minerals. They are intensively leached. Their Suborders and Great Groups are equivalent to Ferralsols, Planosols and Gleysols of FAO.

SPODOSOLS (*-ods*) Soils with a diagnostic spodic horizon corresponding to Podzols (FAO).

ULTISOLS (*-ults*) Soils with a diagnostic argillic (illuvial, rich in clay) horizon having a small base saturation. Their Great Groups correspond to Acrisols and Nitisols (FAO).

VERTISOLS (*-ert*) Soils equivalent to Vertisols of FAO.

1.1.3 Soil Mapping

The basic element of a soil and that of a soil map is the pedon. It is a three-dimensional body having a geographical surface area of 1 to 10 m^2. We usually describe its morphology on a two dimensional vertical cross section of a soil profile, i. e. on the wall of an excavated pit. The positions of individual pedons are usually identified on maps of scale 1:2000 or 1:5000 with abbreviations of important properties. With the pedon classified according to the lowest level of the taxonomic system, we obtain the abstract form - a pedotop. On geographically large scale maps (1:2000 is larger than 1:20000) we approximate

the boundary of the domain of each pedotop either by simple interpolation or with the help of geostatistics. The term polypedon is used to include the variation of pedons within one basic pedotop. The domain of one pedotop typically contains inclusions of polypedons of a neighboring pedotop. In such cases a pedotop is polymorphic. A monomorphic pedotop has no inclusions of neighboring pedotops.

The mosaic structure of pedotops are defined as pedochors or pedocomplexes which are characterized by an areal distribution of individual pedons including their extremes and frequency. In a given pedochor, the occurrence of polypedons frequently depends upon topography, e. g. hydromorphic soils occur in depressions of alluvia while around the depressions at slightly higher elevations of the alluvium semihydromorphic soils occur. And on the next higher terrace, lithogen soils can occur without features of hydromorphism. These gradual transitions within pedochors are called catena. Pedochors are used with scales up to 1:50000. For smaller scales, soil taxons of medium level are used and frequently grouped into pedoregions which contain taxons having similar features.

For studies of soil hydrology, the largest scales of polypedons and those of domains including the lowest level of taxons are most appropriate whenever the heterogeneity of the landscape is described deterministically, In such cases the scale of pedochors can be used for linking soil hydrology to mapping units with certain assumptions and approximations. However, a detailed preliminary study of the mutual relationships between mapping units and soil hydraulic properties is indispensable and the knowledge gained is not simply transferable to other pedochors. Efforts to apply maps of smaller scale (pedoregions) to soil hydrological studies are futile.

1.2 CONCEPTS OF SOIL HYDROLOGY

All studies in soil hydrology eventually have a unique aim - a better understanding and description of hydrological processes. The individual elementary processes of infiltration, redistribution, drainage, evaporation and evapotranspiration are first analyzed and subsequently considered in combination during a particular sequence of events or season. Transport of

solutes is also considered as an integral part of those processes. All such processes occur in soils and under actual meteorological situations. A proper physical understanding of them requires several approximative levels of studies.

As a first approximation we model the soil as a simple, homogeneous porous body temporarily forgetting the existence of horizons within its profile and the horizontal variation of its properties. In some instances a soil profile consisting of two horizons is modeled simply by considering a layer of a homogeneous soil overlain by a second having different hydraulic properties. For studying the behavior of soil water including flow and transport of matter, we use phenomenological (or macroscopic) descriptions. We describe what we can "see" with our apparatuses and we denote the scale where the phenomenological approach is applied as Darcian. Only when the physical interpretation of some phenomena requires a detailed discussion at the microscopic level will we temporarily abandon laws and equations based on a macroscopic scale of observation.

The elementary hydrologic processes for simply modeled soils and for trivial boundary conditions are described by analytical solutions of the basic macroscopic equations. The advantage of analytical solutions is a full understanding of the physical processes. Parallel to such mathematical analyses are carefully conducted experiments performed on repacked soil columns or on model porous materials under precise conditions in the laboratory.

The next level of approximation is the quantification of processes for real soils, i. e. field soils. Although the scale remains Darcian, we speak of it as the pedon scale. At this level the boundary conditions are usually less trivial than those used in the first level, and if they are sufficiently complex, numerical methods are applied to achieve particular solutions. These results, similar to an accurately performed field experiment, are regularly verified by field experimentation. The advantage of numerical simulation is the rapid production of a large number of "computer experiments" which partially substitute for tedious, time-consuming field experiments. Alternatively, numerical procedures allow us to study specific features of a process which are not accessible or readily observed by existing experimental techniques. We

properly interpret the data physically by applying the knowledge we gained at the first approximation level.

From these pedon studies (often called "point scale" studies) we try to extend the results to the larger scale of a field or catchment. This scale, larger than Darcian, is denoted as megascale or catchment scale. At this scale, methods used at smaller scales need to be modified with stochastic characteristics entering our equations and procedures. The stochastic structure of these hydraulic properties of field soils is studied by specific procedures. In some instances we obtain a set of deterministic pedon-scale observations spatially distributed across the field or catchment to define a newly formed stochastic or regionalized variable. In other instances, entirely new approaches are developed applicable only to the megascale.

Analogous to these briefly introduced concepts of soil hydrology, we proceed further into the content of the book.

5 HYDRODYNAMICS OF SOIL WATER

We introduced the concept of soil water potential in Chapter 4 where the system was studied at the equilibrium state. It was characterized by a driving force equal to zero and the value of the total potential being equal at all locations in the soil. Under such conditions, the water flux density is zero and both the soil water content θ and the soil water pressure head h are invariant with time. Here we derive equations describing the water flux when the soil system, not in equilibrium, manifests a total potential Φ not being constant in space.

5.1 BASIC CONCEPTS

The flow of water in soil can be described microscopically and macroscopically. On the microscopic scale, the flow in each individual pore is considered and for each defined continuous pore, the Navier-Stokes equations apply. For their solution we lack detailed knowledge of the geometrical characteristics of individual pores to obtain a solution for the REV. Even with this knowledge, a tremendous effort would be required necessitating voluminous calculations for even a relatively small soil domain. Nevertheless, this type of procedure is often applied in some theoretical investigations where the basic laws of fluid mechanics are invoked. In such studies the real porous system is usually defined by a model assuming great simplification of reality.

The macroscopic or phenomenological approach of water transport relates to the entire cross-section of the soil with the condition of an REV being satisfied. The rate of water transport through the REA is the flux. In order to emphasize the fact that water does not flow through the entire macroscopic areal cross section, the term flux density (or flux ratio, macroscopic flow rate et al.) is used to describe the flow realized through only that portion of the area not occupied by the solid phase and, by the air phase eventually when we deal later on with unsaturated soil. Moreover, we use the term flux density understanding that we actually mean the volumetric water flux density having the dimensions of velocity [LT^{-1}].

Inasmuch as the principal equation derived for this macroscopic approach is Darcy's equation, the scale for which this approach is valid is often denoted as the Darcian scale. For soils, the area of this scale is usually in the range of cm^2 to

m^2. Beyond this scale in either direction, larger or smaller, Darcian scale equations may not be realistic. Unless we state otherwise, equations will be derived and solved mainly for the Darcian scale related to a particular REV.

On the Darcian scale, water flow in soils is comparable to other transport processes such as heat flow, molecular diffusion etc. when the appropriate driving force is defined. For example, when the distant ends of a metal rod are kept at different temperatures, heat flow exists. Similarly, molecular diffusion depends upon a difference of concentration in two mutually interconnected pools. Soil water flow is conditioned by the existence of a driving force stemming from a difference of total potentials between two points in the soil. Laymen mistakenly suppose that the driving force of water flow in an unsaturated soil is related to differences in soil water content. This supposition, valid only for a few specified conditions, generally leads to erroneous conclusions.

Here, we first formulate basic flow equations for the simplest case of flow in a saturated, inert rigid soil. Afterwards, we deal with water flow in a soil not fully saturated with water. This latter type of flow is commonly called unsaturated flow while the former is called saturated flow. To be more precise, we should distinguish the former from the latter flows as those occurring at positive and negative soil water pressures, respectively. If the flow of both air and water in the soil system is simultaneously considered, we speak of two phase flow. Initially, we assume that the concentration of the soil solution does not affect the soil water flow. Subsequently, our discussion is extended to swelling and shrinking soils. Finally, we examine linked or coupled flows together with some specific phenomena of transport at temperatures below 0°C.

All equations that we derive are supposed to be applicable to not only analytical and approximate mathematical solutions of the components of the soil hydrological system but to all deterministic models of soil hydrology.

5.2 SATURATED FLOW

We assume that water is flowing in all pores of the soil under a positive pressure head h. In field situations the soil rarely reaches complete water saturation. Usually it is quasi-saturated with the soil water content $\theta = m P$ where m has values of 0.85 to 0.95 at $h \geq 0$, and P is the porosity. Entrapped air

occupies the volume $P(1 - m)$. And for this discussion of saturated flow, the impact of entrapped air is not considered.

5.2.1 Darcy's Equation

For the derivation of Darcy's equation we shall discuss a simple experiment demonstrated in Fig. 5.1. The soil is placed in a horizontal cylinder connected on both sides with vessels containing water maintained at a constant level in each vessel by an overflow valve. If the water level on the left side is higher than that on the right side, water flows to the right. The rate of discharge $Q = V/t$ is simply measured by the volumetric overflow V in time t. The flux density q [LT^{-1}] (macroscopic flow rate) is

$$q = \frac{V}{At} \tag{5.1}$$

where A is the cross-sectional area of the soil column perpendicular to the direction of flow. Sometimes, the term q is also called the Darcian flow rate. The mean water flow rate (velocity) in the soil pores v_p is

$$v_p = q / P \tag{5.2}$$

5.1

In 1856, Darcy experimentally demonstrated for columns of sand a linear relationship between the flux density q and the hydraulic gradient I_h. In our experiment shown at the bottom of Fig. 5.1

$$q = K_S \frac{\Delta h}{L} = K_S \frac{\Delta h'}{L'} = K_S I_h \tag{5.3}$$

where $\Delta h/L$ or $\Delta h'/L'$ is the hydraulic gradient I_h, Δh the difference between water levels on both ends of the soil column of length L and $\Delta h'$ the difference between water levels in the piezometers separated by the distance L' in the direction of flow. Both Δh and $\Delta h'$ are considered the hydraulic head drop along the soil. Inasmuch as $\Delta h/L$ is dimensionless, K_S has the dimension of q [LT^{-1}]. When we read piezometer levels h_1 and h_2 at elevations z_1 and z_2, respectively, we have

$$q = - K_S \left(\frac{H_2 - H_1}{z_2 - z_1} \right) \tag{5.4}$$

where the total potential head H ($= h + z$) is related to a unit weight of water. In a more general way (5.4) becomes

$$q = - K_S \, grad \, H \tag{5.5}$$

Equation (5.5) states that the flux density is proportional to the driving force of the water flow which is the gradient of the potential. Inasmuch as K_S is a constant for a given soil, we write $\phi^* = K_S H$, and hence,

$$q = - grad \, \phi^* \tag{5.6}$$

where ϕ^* is $K_S H$. The negative sign in the above equations means that water flows in the direction of decreasing potential or against the positive direction of z in Fig. 5.1. The value of K_S depends upon the nature of the soil and is numerically equal to the flow rate when the hydraulic gradient is unity. Values of K_S commonly range from less than 0.1 cm·day^{-1} (10^{-8} m·s^{-1}) to more than 10^2 cm·day^{-1} (10^{-5} m·s^{-1}).

In layered soils we have to specify the direction of the flow relative to that of the layering. When the flow is parallel to the layers, the total flux density is the sum of the flux densities for each of the individual layers, see Fig. 5.2. Hence,

$$q = q_1 + q_2 + q_3 \tag{5.7}$$

For a column of width $d = 1$, length L and thickness b composed of three layers each of thickness b_i, the total flux density for a hydraulic head drop Δh is

$$q = \left(K_1 b_1 + K_2 b_2 + K_3 b_3 \right) \frac{\Delta h}{L} \tag{5.8}$$

Here, the apparent hydraulic conductivity K_S' is the arithmetic mean of the individual values for each layer.

5.2

When water flows perpendicular to the layering, we introduce, analogous to an electrical resistance, the hydraulic resistance of each layer $R_i = L_i / K_{Si}$ having units of time. In Fig. 5.2 the flow combined from the three layers is

$$q = \frac{\Delta h}{R_1 + R_2 + R_3}. \tag{5.9}$$

With the total resistance of the system $R = \Sigma R_i$ we obtain the harmonic mean or the apparent hydraulic conductivity $K_S' = L/R$.

5.3

When the flow is at an angle < 90° to the layers, the difference of K_S in each of the layers causes a change of the direction of streamlines (Zaslavsky and Sinai, 1981, and Miyazaki, 1990), see Fig. 5.3.

5.2.2 Saturated Hydraulic Conductivity

Inasmuch as the soil water potential H can be expressed in three modes, the dimension of the hydraulic conductivity is not necessarily [LT^{-1}]. From (5.5) we obtain for the three dimensions of H three different dimensions of K_S. Although expressing K_S in units of velocity is usually more convenient, any one of the following sets of units is occasionally preferred.

H		grad H		Ks	
J kg^{-1}	[L^{2}T^{-2}]	J kg^{-1} m^{-1}	[LT^{-2}]	s	[T]
Pa	[ML^{-1}T^{-2}]	Pa m^{-1}	[ML^{-2}T^{-2}]	m s^{-1}ρ$_W^{-1}$g^{-1}	[M^{-1}L^{3}T]
m	[L]	dimensionless		m s^{-1}	[LT^{-1}]

The empirical, intuitive derivation of Darcy's equation (5.5) can be theoretically justified from Navier-Stokes equations applied to an REV of a model of a porous medium and scaled with a characteristic length. In order to obtain (5.5), inertial effects were neglected and the density and viscosity of water were assumed invariant (Bear, 1972; Whitaker, 1986). Scheidegger (1957) showed that K_S should be considered a scalar quantity for isotropic soils, and a tensor of rank 2 for anisotropic soils with the value of K_S dependent upon the direction of flow. When the tensor K_S is assumed to be symmetric, its principal axes, defined by six values, are identical to those of an ellipsoid of conductivity. If the gradient of the potential is not in the direction of a principal axis, the direction of flow is different from that of the gradient.

5.4

From a theoretical treatment we can obtain a physical interpretation of the hydraulic conductivity. We develop here a modified and simplified model of Kozeny (cf. Scheidegger, 1957) consisting of a bundle of parallel capillary tubes of

uniform radius. We assume that the soil and the model are identical with respect to porosity P, specific surface A_m [L^{-1}] and water flux density q [LT^{-1}], see Fig. 5.4. The mean flow rate v_p in a capillary of radius r is described by Hagen-Poiseuille's equation

$$v_p = \frac{\rho_w g r^2}{8\mu} I_h \tag{5.10}$$

where g is the acceleration of gravity [LT^{-2}], ρ_w the density of water [ML^{-3}], μ the dynamic viscosity [$ML^{-1}T^{-1}$] and I_h the hydraulic gradient [dimensionless]. With n being the number of capillaries of unit length x, the porosity of the model is

$$P = n\pi r^2 x / V_u \tag{5.11}$$

where V_u is the unit volume and the specific surface is

$$A_m = 2n\pi r x / V_u \tag{5.12}$$

From (5.11) and (5.12) we obtain

$$r = \frac{2P}{A_m} \tag{5.13}$$

And, from (5.2) and (5.10) we obtain

$$q = \frac{1}{2}\frac{\rho_w g}{\mu}\frac{P^3}{A_m^2} I_h \tag{5.14}$$

Because soil pores are irregularly shaped and mutually interconnected, a shape factor c replaces 1/2 in (5.14). Letting

$$K_p = \frac{cP^3}{A_m^2} \tag{5.15}$$

we obtain

$$q = K_p \frac{\rho_w g}{\mu} I_h \tag{5.16}$$

which is identical to (5.3). Because the term K_p relates to the flow of any fluid through a soil, it is called the permeability [L^2]. The unusual dimension of K_p represents the cross-sectional area of an equivalent pore. Although now almost obsolete, the historical unit of 1 Darcy = 1 μm^2 was used for describing permeability.

Inasmuch as flow channels in the soil are curved compared with those of a capillary model, a tortuosity factor τ introduced in (5.15) yields the Kozeny equation

$$K_p = \frac{cP^3}{\tau A_m^2} \tag{5.17}$$

The tortuosity τ is the ratio between the real flow path length L_e and the straight distance L between the two points of the soil. Because $L_e > L$, $\tau > 1$. In a monodispersed sand manifesting a value of $\tau \approx 2$, the flow path forms approximately a sinusoidal curve (Corey, 1977).

Equations identical or of similar type to (5.17) have been derived by many authors. If a model of parallel plates is used instead of capillary tubes and the slits are oriented in the direction of the laminar flow, we obtain the mean flow rate

$$v_p = \frac{\rho_w g d^2}{3\mu} I_h \tag{5.18}$$

where $2d$ is the distance between the plates. When B is the width of the plates, $P = 2ndBx/V_u$ and $A_m = 2nx(2d + B)/V_u$. Taking $x = 1$ and $B = 1$, we obtain $d = P(A_m - 2P)$ and hence,

$$K_p = \frac{cP^3}{\tau(A_m - 2P)^2} \tag{5.19}$$

A compromise between (5.17) and (5.19) is the Kozeny-Carman equation

$$K_p = \frac{P^3}{5A_m^2(1-P)^2} \tag{5.20}$$

derived in detail by Scheidegger (1957).

From (5.3) and (5.16) the relationship between K_S and any formulation of K_p is

$$K_S = K_p \frac{\rho_w g}{\mu} \qquad (5.21)$$

Kozeny's equation shows that K_S is sensitive to porosity. However, in his model the pore radii are considered uniform while those in real soils have broad distributions. For real soils, we subdivide the pores according to their radii into j categories each having an equivalent radius r_j. For $r_j > r_{j+1}$ the flux in each category $q_j(r_j^4, n_j)$ where n_j is the percentage of the j-th category in the whole soil, $q_j >> q_{j+1}$. Total flux $q = \Sigma\, q_j$ as shown for parallel layering. Thus, let us assume for $j = 1$, the percentage of the category of largest pores is eliminated by compaction. Although the porosity may be only marginally reduced, the value of K_S may be reduced by orders of magnitude. It is logical, therefore, that aggregation of a soil may increase K_S by orders of magnitude, yet the porosity may remain nearly the same. And, vice versa, soil dispersion or disaggregation substantially decreases K_S. For example, in a loess soil, the saturated hydraulic conductivity of its surface after a heavy rain decreases 3 to 4 orders of magnitude compared with its original value owing mainly to two processes - disaggregation and the blockage of pores by the released clay particles (McIntyre, 1958). Compaction of soil in the A-horizon and in the bottom of the plowed sub horizon causes a much greater decrease of K_S than that predicted from a decrease of porosity in the simple Kozeny equation because compaction reduces primarily the content of large soil pores associated with values of pressure head h = 0 to -100 cm.

Although the textural class of a soil may have a large influence on the value of K_S, any attempt to establish a correlation between the two attributes usually fails. Only for those soils and soil horizons of the same genetic development occurring in the same region and being similarly managed will a correlation between texture and K_S be manifested. On the other hand, a few generalities may exist. For example, the smallest values of K_S in each of the main textural classes can be approximated. In sandy soils, the minimum value of K_S is about 100 cm·day^{-1}, in silty loams about 10 cm·day^{-1} and in clays about 0.1 cm·day^{-1}. In

peats, K_S decreases with an increasing degree of decomposition of the original organic substances. When the degree of decomposition of a peat is about 40 to 50%, the value of K_S diminishes to values of K_S typical of unconsolidated clays. Extreme drainage and concomitant drying of peat soils causing compaction and an increase of soil bulk density also reduce the magnitude of K_S. Moreover, because this drying increases hydrophobism, entrapment of air during wetting is enhanced and contributes even further to the decrease of K_S.

In loams and clays, the nature of the prevalent exchangeable cation plays an important role relative to the value of K_S, see Fig. 5.5. In Vertisols, an increase of the percentage of exchangeable sodium (ESP) is accompanied by a decrease in K_S when the ESP reaches 15 to 20%, provided that the soluble salt content of the soil water is small. For example, with the electrical conductivity of the soil paste EC being 1 mS cm^{-1} or less, the value of K_S can decrease two or three orders of magnitude. On the other hand, even for the same soil having a large ESP, if the concentration of soluble salts is increased substantially to an EC value of about 8 mS cm^{-1} or more, the K_S value is not significantly affected. In addition to the coupled role of soluble salt content and ESP, the sodium adsorption ratio (SAR) is of great importance to the dynamics of the variability of K_S (Russo and Bresler, 1977). These variations are closely related to the degree of flocculation or peptization of the soil colloidal particles that can be quantified with the value of the ζ-potential derived from double layer theory. Applying this theory, the decrease in K_S owing to the action of rain water (very small EC) is easily predicted for soils having large SAR values. These predictions are not necessarily successful for soils that differ pedologically. For example, a solution of high SAR value percolating through an Oxisol does not decrease the value of K_S even after reducing the solute concentration because the abundant free iron oxides prevent peptization and disaggregation of the soil particles. The value of K_S also depends upon the composition of the clay fraction. It decreases in the order kaolinite, illite and montmorillonite. And, soil organic matter has a profound impact upon the magnitude of K_S, owing to its cementing action that promotes aggregate stability. Generally, there are many factors influencing the value of K_S that are usually not considered in simplified models.

Soils classified according to their values of K_S are

very low permeability	$K_S < 10^{-7}$ m s^{-1}
low permeability	$10^{-7} < K_S < 10^{-6}$ m s^{-1}

medium permeability	$10^{-6} < K_S < 10^{-5}$ m s^{-1}
high permeability	$10^{-5} < K_S < 10^{-4}$ m s^{-1}
excessive permeability	$K_S > 10^{-4}$ m s^{-1}

Geological materials are similarly classified as

compacted clays	$10^{-11} < K_S < 10^{-9}$ m s^{-1}
gravel	$10^{-1} < K_S < 10^{1}$ m s^{-1}

All such classification schemes above are problematical. For soils in a certain region, a more appropriate classification would be based upon the frequency distribution of K_S. Based upon that frequency distribution, we can identify subregions where a particular range of K_S is expected.

When values of K_S are considered relative to their position within a soil profile, soils are grouped into these seven classes.

1. K_S does not change substantially in the profile.
2. K_S of the A-horizon is substantially greater than that of the remaining soil profile and no horizon of extremely low K_S exists.
3. K_S gradually decreases with soil depth without distinct minima or maxima.
4. K_S manifests a distinct minimum value in the illuvial horizon or in the compacted layer just below the plow layer.
5. Soil of high permeability with its development belonging to one of the first four classes covering the underlying soil of very low permeability.
6. Soil of very low permeability with its development belonging to one of the first four classes covering the underlying soil of very high permeability.
7. K_S changes erratically within the profile owing to extreme heterogeneity in the soil substrata.

The influence of the temperature upon the value of K_S can be examined with (5.21). Inasmuch as ρ_W is negligibly influenced by temperature, changes of $K_S(T)$ depend primarily upon the viscosity $\mu(T)$.

5.2.3 Darcian and Non-Darcian Flow

We have already mentioned that Darcy's equation is valid only for small rates when the inertial terms of the Navier-Stokes equations are negligible. For engineering purposes the upper limit of the validity of Darcy's equation given by (5.3) through (5.6) is indicated by the critical value of Reynolds' number for porous media

$$\mathrm{Re} = \frac{qd\rho}{\mu} \tag{5.22}$$

where d denotes length. In sands, d is the effective diameter of the particles, or with some corrections, the effective pore diameter. Sometimes d is related to the permeability of the sand, e. g. $d = K_p^{1/2}$. However, in all soils other than sands, d is not at all definable and hence, (5.22) is not applicable. The difficulty in defining d is manifested by controversy in the literature regarding the assignment of critical values of Re. Most frequently, critical values of Re have been reported to range from 1 to 100. In this post linear region, the flow is often described by the Forchheimer equation (Bear, 1972)

$$\frac{dH}{dx} = aq + bq^2 \tag{5.23}$$

where a is the material constant analogous to K_S and b is functionally dependent upon the water flux density. This non linearity is caused primarily by inertia and by turbulence starting only at very large values of flux density, see Fig. 5.6. A more detailed theoretical discussion is given by Cvetković (1986).

5.6

Deviations from Darcy's equation have also been observed in laboratory experiments for very small flux density values. We define, therefore, the pre linear region of flow where q increases more than proportionally with I_h, see Fig. 5.6. This deviation from Darcy's equation, most often observed within pure clay having very large specific surfaces (e. g. 10^2 m^{2}g^{-1}), has been explained by the action of three factors: a) Clay particles shift and the clay paste consolidates owing to the imposed hydraulic gradient and the flow of water, b) It is theoretically assumed that the viscosity of water close to the clay surfaces is different than that of bulk water or that in the center of the larger soil pores. According to Eyring's molecular model where the viscosity depends upon the activated Gibbs free energy, the first two to five molecular layers have a distinct increased viscosity. Owing to the great value of the specific surface in clays, the contribution of the first molecular layers to the alteration of averaged viscosity

may not be negligible. c) The coupling of the transfer of water, heat, solutes et al. may also contribute to the existence of the pre linear region (Swartzendruber, 1962; Kutílek, 1964, 1972 and 1978; Nerpin and Chudnovskij, 1967).

Deviations from Darcian flow are not frequently described or observed, and the post linear region is only rarely reached in sands and gravelly sands. There is not yet any field experimental evidence of the existence of a pre linear region. Darcy's equation is, therefore, either exact or at least a very good approximation entirely adequate for soil hydrology.

5.2.4 Measuring K_S

Saturated hydraulic conductivity is one of the principal soil characteristics and for its determination, only direct measurement is appropriate. Indirect methods, derived from soil textural characteristics which are sometimes combined with aggregate analyses, generally do not lead to reliable values. Considering soil texture as an example, soil water flow is totally independent from the laboratory procedure of dispersing, separating and measuring the percentage of "individual" soil particles which do not even exist "individually" in natural field soils. It has been shown in section 5.2.2 that the value of K_S is closely related physically to the porous system within a soil. Inasmuch as a quantitative description of this porous system is much more difficult than the measurement of K_S, direct measurement of K_S is preferred. When K_S is ascertained by water flux density and potential gradient measurements, we will speak about the determination of K_S. In order to avoid misunderstanding, when additional assumptions are used to evaluate these two quantities somewhat less directly, we will speak about the estimation of K_S.

Measuring is realized either in the laboratory on soil core samples previously taken from the field, or directly in the field without removing a soil sample. Field methods are preferred. They provide data that better represent the reality of water flow in natural conditions. Their main disadvantage is the lack of rigorous quantitative procedures for measuring soil attributes in the majority of field tests. For laboratory measurements, the size of the REV should be theoretically estimated in order that an appropriate soil core sampler be selected. In practice, because the REV is rarely determined, a standard core or cylinder size is used for most soils. As a result, larger numbers of samples are taken with appropriate statistical evaluation of the data in order to partly reduce the error

associated with samples having smaller volumes than the REV. In soils without cracks and frequently occurring macropores a soil sample volume of 200 to 500 cm^3 is assumed satisfactory. In subsoils, a 100 cm^3 sample will sometimes suffice. Methods relying on "undisturbed" core samples are generally not applicable in stony soils, in forests and in soils that crack excessively upon drying.

5.7

In the laboratory, the test is usually performed in a way similar to that demonstrated in Fig. 5.1. When both elevations of the water level are kept constant, i. e. in the vessel before water passes the soil ("upper level") and in the vessel after water has passed through the soil ("lower level"), (5.1) and (5.3) are applied. Apparatuses so constructed are usually called constant head permeameters. More frequently, the upper water level is allowed to fall, see Fig. 5.7. The fall of the water level dh in the measuring tube above the soil sample relates to the flux of water through the soil in time dt. Equating the two volumes, that moving in the measuring tube and that moving through the soil, we have

$$-A_1\,dh = A_2 q\,dt \tag{5.24}$$

where A_1 is the cross-sectional area of the tube above the soil and A_2 is the cross-sectional area of the soil. Substituting q from (5.3) into (5.24) and recognizing that Δh in (5.3) is the total potential head difference h in Fig. 5.7, we have

$$\frac{A_1 L}{A_2 K_S}\int_{h_0}^{h_1}\frac{dh}{h} = -\int_0^{t_1} dt \tag{5.25}$$

After integrating and rearranging

$$K_S = \frac{A_1 L}{A_2 t_1}\ln\left(\frac{h_0}{h_1}\right) \tag{5.26}$$

The method is sometimes modified by having $A_1 = A_2$ and by keeping the bottom vessel without an overflow. Construction details of these apparatuses, usually referred to as falling head permeameters, are given in Klute and Dirksen (1986).

In the field, we generally deal with two cases relative to the determination of K_S. In the first case, a water saturated zone is formed by an unconfined aquifer close to the surface with the ground water level being not deeper than about 1.5 m. In the second case, the soil is not fully saturated.

There exists a number of field methods for determining K_S in the saturated zone. Among them, the auger-hole method and the piezometer method are the most commonly practiced.

In the auger-hole method, a hole is drilled to a depth well below the ground water level. After the water from the hole is rapidly pumped out, the rate of rise of the water level in the hole is registered. A general equation for the computation of K_S is simply

$$K_S = C \frac{dz}{dt} \tag{5.27}$$

where z is the depth of the water level in the hole measured from the hydrostatic ground water level in the soil and C is the shape coefficient dependent upon the geometry of the test. In practice, the derivative in (5.27) is replaced by the differences $\Delta z/\Delta t$ and the coefficient C is evaluated , e. g. according to the potential theory by Ernst (1950) quoted in Maasland and Haskew (1957). Except at the extreme bottom of the hole, it is assumed that the flow paths of water in the soil are perpendicular to the walls of the hole. In order that this assumption be fulfilled, pumping should not be repeated in short sequences of time. Estimation of C for less restrictive geometrical conditions has been described by Boast and Langbartel (1984).

The piezometric method is similar to the auger-hole method except that a tube driven into the augered soil serves as a lining for the hole. The rate of the rise of the water level in the lined hole is measured after pumping a portion of the water from the hole. The lining prevents inflow except through the bottom of the hole. For isotropic soils, K_S is computed from

$$K_S = \frac{\pi r^2}{C\,\Delta t} \ln\left(\frac{z_1}{z_2}\right) \tag{5.28}$$

where r is the radius of the tube inserted into the hole, z_1 and z_2 are the depths of water levels in the hole measured from the hydrostatic ground water level during the time interval Δt. The shape factor $C = 5.6r$ for a flat bottom and $C = 9$ for a hemispherical bottom. Note the similarity between (5.28) and (5.26). The falling head permeameter method modified here with a shape factor C applies to the piezometer method. When the lining does not reach the bottom of the hole, water penetrates additionally from the sides, and the value of the shape factor C increases in relation to L/r where L is the height of the unlined portion of the hole (Smiles and Youngs, 1965).

The piezometric method is ideally suited to measure K_S of anisotropic soils. Two measurements are required. For the first measurement, the lining reaches to the bottom of the hole and we compute with (5.28) the product of the vertical and horizontal hydraulic conductivities, K_V and K_H. In (5.28), K_S is replaced by $(K_V K_H)^{1/2}$ and we assume that the main axes of the hydraulic conductivity tensor are vertical and horizontal. For the second measurement the hole, deepened by the value L without pushing the lining tube deeper, allows inflow into the hole through both the unlined wall of height L and through the bottom. With a new shape factor C_2 in (5.28), the values of K_V and K_H, respectively, are simply calculated with data from the second experiment. A detailed description of methods of measurement of K_S in the field is given by Amoozegar and Warrick (1986). If the saturated soil or aquifer is of great thickness and the locality allows installation of several observation wells, pumping tests can be performed in order to obtain K_S. This method which deals with ground water hydraulics is frequently described in detail in the literature. Data obtained from these pumping tests are not generally compatible with data determined by the auger-hole method representing a weighted average K_S value in the domain of the cone of depression compared with the "point" data of the auger hole method.

The task of measuring K_S in an unsaturated zone is more difficult. Infiltration tests are most frequently used to measure K_S of the topsoil or other horizons near the soil surface. The value of K_S is estimated from readings of cumulative infiltration as a function of time. Alternatively, after a quasi-steady state infiltration rate is reached, its value together with that of the hydraulic gradient estimated from tensiometers installed at two or more depths are used in (5.5) to calculate the value of K_S. The details will be discussed in Chapter 6.

The auger-hole method is commonly modified to determine K_S below the soil surface of an unsaturated soil. Because the zone is not saturated, the modified procedure is opposite to that dealing with a saturated zone. Instead of water being removed from the saturated soil, water is poured into the hole from a marriotte flask. After a relatively short time of 15 to 30 minutes, quasi- steady flow is reached. The steady water flux density q is measured together with the constant height h of the water level above the bottom of the hole. Amoozegar (1989) recommends that K_S be calculated according to Glover's solution

$$K_S = \frac{q\left[\sinh^{-1}(h/r) - \left(r^2/h^2 - 1\right)^{1/2} + r/h\right]}{2\pi h^2} \qquad (5.29)$$

where r is the radius of the hole. This procedure is called the constant head well permeameter method. A similar device is the so-called Guelph permeameter (Reynolds and Elrick, 1985).

5.3 UNSATURATED FLOW IN RIGID SOILS

By the term rigid soil we designate soils that do not change their bulk volume with a change of water content. We assume that unsaturated flow in soils is governed by the same laws that apply to saturated flow. For unsaturated flow we must consider the fact that a portion of the soil pores filled by air could indeed resaturate or drain. In our discussion of unsaturated flow, capillarity will be quoted as well as the term capillary rise frequently used in the literature. However, general mathematical formulations of physical phenomena should be independent of such simplifying ideas as soil capillaries and consequently, when we mention capillarity, it is just for the sake of modeling approximately some effects occurring in real soils.

5.3.1 Darcy-Buckingham Equation

5.8

A simple example of unsaturated flow demonstrated in Fig. 5.8 is analogous to the examples of experiments with saturated flow. The cylinder containing the soil has small openings within its walls leading to the atmosphere. Semipermeable membranes, permeable to water but not to air, separate the soil from free water on both sides of the cylinder. The pools of water are connected to the cylinder with flexible tubes. Full saturation of the soil is first achieved when both pools, lifted to the highest point of the soil, displace the soil air

through the openings on the top side of the cylinder. At this moment, there is no flow in the system and the soil is assumed water saturated. With the pool on the left side of the cylinder lowered to the position h_1 and the pool on the right side to position h_2, air enters into the soil through the openings as the soil starts to drain in a manner similar to a soil placed on a tension plate apparatus. The soil on the left side of the cylinder will be drained to a lesser extent than that on the right side with the soil water content distribution from left to right being nonlinear. Although water flows from the left pool to the right pool, the rate of flow is reduced significantly compared with that when the soil is water saturated. If the water level in each of the pools is kept at a constant elevation with time, steady flow will eventually be reached with the water content at each point within the soil remaining invariant. At this time, the flux density q will depend upon the hydraulic gradient and be governed by an equation similar to (5.3)

$$q = -K\frac{\Delta h}{L} \qquad (5.30)$$

where K is the unsaturated hydraulic conductivity [LT^{-1}]. Inasmuch as the soil is not saturated and flow occurs primarily in those pores filled with water, the value of K will be smaller than that of K_S for the same soil. As for saturated flow we commonly take the potential related to he weight of water, i. e. in units of pressure head. For the majority of practical problems, all components of the total potential except those of gravity and soil water are neglected. Hence, (5.30) rewritten to allow the hydraulic conductivity to be a function of the soil water potential head h is

$$q = -K(h)\frac{dH}{dz} \qquad (5.31)$$

and for two and three dimensional problems

$$q = -K(h)\,grad\,H \qquad (5.32)$$

Equation (5.33) is equivalent to Darcy's equation, and because Buckingham (1907) was the first to describe unsaturated flow dependent upon the potential gradient, equations such as (5.31) and (5.32) are called Darcy-Buckingham equations. The unsaturated hydraulic conductivity K is physically dependent upon the soil water content θ because water flow is realized primarily in pores

filled with water. Because the relationship $\theta(h)$ is strongly influenced by hysteresis, $K(h)$ is strongly hysteretic. On the other hand, it follows from percolation theory that $K(\theta)$ is only mildly hysteretic.

Examples of $K(\theta)$ and $K(h)$ demonstrated in Fig. 5.9, show that the more permeable soil at saturation does not necessarily keep its greater permeability throughout the entire unsaturated region. It is also evident in Fig. 5.9 that the hysteretic behavior of $K(h)$ demands that, for a given value of h, the value of K is greater for drainage than for wetting.

The Darcy-Buckingham equation is adequate for describing unsaturated flow only if the soil water content is not changing in time. Unfortunately, this is seldom the case. When θ and q alter in time, we must combine (5.31) with the equation of continuity. The equation of continuity relates the time rate of change of θ to the spatial rate of change of q in a small elemental volume of soil. The resulting differential equation is strongly non-linear and its solution even for simple conditions is most difficult. Generally, (5.31) is in itself not satisfactory for the solution of such hydrologically important processes as evaporation, infiltration, drainage, subsurface flow etc. Exceptional situations or highly simplified flow conditions are usually the only problems described by the sole use of (5.31).

5.3.2 Unsaturated Hydraulic Conductivity

We distinguish two approaches for a physical interpretation of the measured hydraulic conductivity K. The first is based on the direct application of the Kozeny equation. The second uses the soil water retention curve to quantify the pore size distribution. With this quantification the Kozeny equation is used for sub-groups of pores. In addition to these two physical approaches, empirical formulations of $K(h)$ are used to merely express observed relationships.

Let us first apply the Kozeny equation. Inasmuch as only a portion of the pores is filled with water in an unsaturated soil, we replace the porosity P by the soil water content θ. We assume that the value of the tortuosity τ is described by Corey (1954) as

$$\frac{\tau_s}{\tau(\theta)} = \left(\frac{\theta - \theta_r}{P - \theta_r}\right)^2 \qquad (5.33)$$

which is valid for sands where τ_S is the tortuosity in the saturated soil, $\tau(\theta)$ the tortuosity in the soil having water content θ and θ_r a residual water content. When it is assumed that the tortuosity owing to a change of soil water content is ignored in (5.17), Leibenzon (1947) derived the following expression

$$\frac{K}{K_s} = \left(\frac{\theta - \theta_r}{P - \theta_r}\right)^n \qquad (5.34)$$

where the exponent n should have values ranging from 3.3 to 4. Averianov (1949) proposed that $n = 3.5$ is a good robust estimate. The value of exponent n is related to the pore size distribution and thus to the soil water retention curve SWRC, see Brooks and Corey (1964) who recommended $n = 2/\lambda + 3$ with λ read from (4.42) when P is replaced by θ_S in (5.34). Later on, Russo and Bresler (1980) found that values of 1 or 2 fit better than 3 in the exponent n. Childs and Collis-George (1950) obtained the equation

$$K = \alpha \frac{\theta^3}{A_m^2} \qquad (5.35)$$

which is comparable to that of Deryaguin et al. (1956)

$$K = \alpha \frac{A_m d^3}{2\mu} \qquad (5.36)$$

provided that we assume smooth walls. At small soil water contents and in soils having rough walls, the power function $K \alpha \theta^n$ remains but the exponent $n \neq 3$. A physical interpretation can be obtained using a fractal model of wall roughness (Toledo et al., 1990) The identity of both equations (5.35) and (5.36) is reached when the average thickness of the water film d is taken as functionally dependent upon θ for a given specific surface A_m. In both equations α is an empirical coefficient.

Inasmuch as $\theta(h)$ exists, the dependence of K upon h is also deducible with many empirical formulae quoted in the literature.

Gardner (1958) modified Wind's (1955) empirical proposal

$$K = a\,h^{-m} \tag{5.37}$$

to the relationship

$$K = \frac{a}{|h|^m + b} \tag{5.38}$$

applicable to $h = 0$ where a, b and m are empirical coefficients. Note that for $h = 0$ in (5.38), $a/b = K_S$.

Gardner's exponential relationship (1958)

$$K = K_S \exp(ch) \tag{5.39}$$

is frequently used in analytical solutions. If K/K_S is plotted against h on semi-log paper, a straight line is obtained. This relation usually fits the experimental data well in the range from $h = 0$ ($\theta = \theta_S$) to a certain h_{lim}, see Fig. 5.9, top right. For soils manifesting a distinct air entry value h_A, Gardner and Mayhugh (1958) modified (5.41) to

$$K = K_S \exp\left[c\left(h - h_A\right)\right] \tag{5.40}$$

The value of the empirical coefficient c with dimension $[L^{-1}]$ is related to soil texture. and most frequently, $c = 0.1$ to 0.01 cm^{-1}. For δ-function soils in the Green and Ampt approximation of infiltration the value of c is numerically equivalent to the soil water pressure head $|h_f|$ at the wetting front, see Chapter 6. Both (5.39) and (5.40) have been broadly used in analytic and semi-analytic solutions , especially for steady flow problems as we show with some examples in Chapter 6 and as was fully reviewed by Pullan (1990).

Because (5.39) and (5.40) are valid in the wet range, (5.38) might be preferred in the dry range For $h < h_{lim}$, we must use c_2 different from c to extend the applicability of the equation to the dry range. $K(h)$ is often defined as a composite function. For example, the range of $h_A > h > h_{lim}$, (5.39) applies and for $h < h_{lim}$, (5.37) or (5.38) applies in order to simulate the entire soil water regime in some instances.

From studies of capillarity in sands, Brooks and Corey (1964) obtained the frequently used relationship

$$\frac{K}{K_S} = \left(\frac{h_A}{h}\right)^m \tag{5.41}$$

where m depends upon the pore size distribution. Usually $m = 3$ to 20.

Physical interpretation of $K(\theta)$ or $K(h)$ must include in addition to the total porosity, the distribution of the pore sizes. Recognizing from (5.10) that the flow rate in a cylindrical capillary is $v_p\,(r^2)$, drainage of the largest pores drastically reduces the value of K in spite of the relatively small volume of those pores. Childs and Collis-George (1950) were the first to propose a method relating $K(\theta)$ to a pore size distribution function $f(r)$. Using the soil water retention curve to reflect $f(r)$, they obtained (5.35) as a simplified result. Their general approach attracted attention and was further developed and modified. We show those developments here.

In its simplest form the porous system is composed of j categories of pores with $j = 1$ for the category of smallest pores. In each category the pore radii are in ranges r_{j-1} to r_j. In each category the flux is $q_j(\bar{r}_j^4, n)$ where $\bar{r}_j$ is the mean radius and n is the percentage of the category and frequently $q_{j-1} < q_j$ even if $n_{j-1} > n_j$. Assuming $\nabla H = -1$, the unsaturated hydraulic conductivity $K = \sum q_j$. When the soil is only partially saturated with water, contributions of fluxes q_j, q_{j-1} et al. from the larger , empty pores of radii j, (j-1) et al. do not exist, see Fig. 5.10. In a more exact derivation, we start with the mean flow rate v_p in pores of radius r according to the Hagen-Poiseulle equation

$$v_p(r) = a r^2 I_h \tag{5.42}$$

where $a = \rho_W g / 8\mu$, see (5.10). The flux density in a porous system with a continuous distribution function of pores $f(r)$ and a tortuosity τ is

$$q = \frac{1}{\tau}\int_0^r v_p(r) f(r)\,dr. \tag{5.43}$$

Or, with (5.42) for $I_h = 1$, $q = K$ and

$$K = \frac{1}{\tau}\int_0^r a r^2 f(r)dr. \tag{5.44}$$

When $f(r)dr$ is approximated by $d\theta_E(h)$, i. e. by the SWRC and for the relation between the pore radius and the pressure head ($r = c/h$), we obtain

$$K = \frac{ac}{\tau}\int_0^{\theta_E} \frac{1}{h^2(\theta_E)} d\theta_E(h). \tag{5.45}$$

For relative hydraulic conductivity K_r

$$K_r = K / K_S \tag{5.46}$$

and with the tortuosity from (5.33) modified to

$$\tau_S / \tau = \theta_E^b, \tag{5.47}$$

we have

$$K_r = \theta_E^b \int_0^{\theta_E} \frac{d\theta_E}{h^2(\theta_E)} \Big/ \int_0^1 \frac{d\theta_E}{h^2(\theta_E)} \tag{5.48}$$

Various authors have not found a unique interpretation for exponent b in the above equation. Marshall (1958) and Millington and Quirk (1961) defined b as the probability of occurrence of continuous pores. For isotropic and homogeneous media $b = 2P_f$ with P_f denoting that portion of the porosity within which water is flowing. Marshall assumed $P_f = 1$ and hence, b was 2. Millington and Quirk used P_f as 2/3 and hence, b was 4/3. Burdine (1953) interpreting the tortuosity with (5.33) evaluated b as 2.

Inasmuch as the microscopic pore size distribution is used to characterize the macroscopic flux in a soil, Mualem (1976) classified such models as microscopic models. After evaluating about 50 soils on a macroscopic scale, Mualem decided that b was 1/2. Hence, (5.48) becomes

$$K_r = \theta_E^{0.5}\left[\int_0^{\theta_E} \frac{d\theta_E}{h(\theta_E)} \Big/ \int_0^1 \frac{d\theta_E}{h(\theta_E)}\right]^2. \tag{5.49}$$

If the van Genuchten soil water retention curve (4.43)

$$\theta_E = \frac{1}{\left[1+\left(\alpha|h|\right)^n\right]^m} \tag{5.50}$$

and (5.48) are combined, we obtain

$$K_r\left(\theta_E\right) = \theta_E^b\left[1-\left(1-\theta_E^{1/m}\right)^m\right]^2 \tag{5.51}$$

with $m = 1 - c/n$ and $n > 1$. For the model of Burdine, $a = 1$, $b = 2$ and $c = 2$. For the model of Mualem, $a = 2$, $b = 0.5$ and $c = 1$. Let us note that Mualem's database consisted mainly of repacked laboratory soils and $b = 0.5$ does not hold for all field soils where the deviation may vary from less than -10 to more than 10 (van Genuchten et al., 1989).

Mualem's model of $K(h)$ is

$$\frac{K(h)}{K_S} = \frac{\left\{1-\left(\alpha|h|\right)^{n-1}\left[1+\left(\alpha|h|\right)^n\right]^{-m}\right\}^2}{\left[1+\left(\alpha|h|\right)^n\right]^{m/2}} \tag{5.52}$$

Similarly, using the soil water retention curve $\theta_E = (h_A/h)^\lambda$ of Brooks and Corey (4.42) the relative hydraulic conductivity is

$$\frac{K(\theta_E)}{K_S} = \theta_E^{a+b/\lambda} \tag{5.53}$$

and

$$\frac{K(h)}{K_S} = \left(\frac{h_A}{h}\right)^{a+b/\lambda} \tag{5.54}$$

For the model of Childs and Collis-George, $a = 2$ and $b = 2$. For that of Burdine, $a = 2$ and $b = 3$. For that of Mualem, $a = 2$ and $b = 2.5$.

The exponent $(a + b/\lambda)$ in (5.54) is identical to the exponent m in (5.41). Although the value of the exponent should theoretically be in a narrow range between 2.5 and 4.5, experimental data yield values that extend to about 11. This

discrepancy can be explained by the over-simplification of the porous body in the model. In the derivation of the above equations, several approximations were made. First, the soil porous system was modeled by a bundle of cylindrical capillary tubes. Second, the pore size distribution function was approximated from the soil water retention curve. And third, the value of b was empirically evaluated. However, in spite of these approximations for the derivation of $K(\theta_E)$ and $K(h)$, the most problematic is the proper interpretation of the soil water retention curve close to θ_S.

A formal sensitivity analysis of (5.52) by Wösten and van Genuchten (1988) showed that differences in K_r increase with a decrease in h (i. e., with the soil drying) as the parameter α is altered, see Fig. 5.11. On the other hand, the influence of the exponent n also brings about a great potential error in the wet region. In Fig. 5.11, θ_E has been replaced by θ with the soil water retention curve (4.43) having the form

$$\theta = \theta_r + \frac{\theta_s - \theta_r}{\left[1+\alpha|h|^n\right]^m}. \qquad (5.55)$$

5.11

Additional sensitivity analyses made by Šír et al. (1985) and Vogel and Císlerová (1988) show the role of an error $\delta h(\theta_E)$ in the experimental determination of $h(\theta_E)$. If $\delta h(\theta_E)$ is a constant in the range $0 \le \theta_E \le 1$, the absolute error of $K(\theta)$ rises steeply with an increase of θ_E.

When the soil porous system is characterized by a bi-modal pore size distribution curve (Fig. 4.19), the relation K(h) shows two distinct regions. For $0 > h > h_1$, only the by-pass pores belonging to the secondary peak are considered with Mualem's model applied to the soil water retention curve of the inter-pedal (by-pass) pores. For $h < h_1$ we use the remaining portion of the SWRC representing only the intra-pedal (matric) pores, see Fig. 5.12 and Othmer et al. (1991). Hence, two matching factors are needed. For the region $0 > h > h_1$ the matching factor is K_S. For the region $h < h_1$ it is a measured value of $K(h < h_1)$. Although this mechanistic separation of the two porous systems uses the same basic equations, the accelerated fluxes through the by-pass pores are conveniently described.

5.12

Up to now we have discussed the problems related to $K(\theta)$ in a wet soil. In a dry soil, the probable errors in modeling $K(\theta)$ are related to θ_r. The residual soil

water content θ_r in θ_E of (5.50) and further on in other $K(\theta)$ models leads to $K(\theta \le \theta_r) = 0$. This zero value of hydraulic conductivity for $\theta > 0$ is in agreement with our description of SWRC in Section 4.3 where we used θ_{Wr} to denote the boundary between coherent and incoherent water phase distributions. However, we have shown in the same Section 4.3 that θ_r is obtained as a fitting parameter which we are not allowed to interpret physically. Thus, the physically observed θ_{Wr} in $K(\theta)$ may not coincide with θ_r obtained by fitting (4.42) or (4.43) to experimental SWRC data. A simple method for independently estimating θ_{Wr} for $K(\theta)$ models has not yet been proposed and tested on a broad scale.

Macropores play a special role in the flow of water especially during infiltration. When the soil water pressure is positive or when an unsaturated soil is ponded with water, water flows in the so-called "macropores". The mechanism of the flow in this case may be different from that of the capillary porous system. Water may flow either along the walls of the pores like a thick film, or through the entire cross-sectional area of the pore. When water conduction in cracks is combined with absorption, the kinetic wave approximation (German and Beven, 1985) can be used. The flux density is restricted just to macropores and it is generally reduced by absorption. The theory describes the transformation of both flux density and front velocity when water is transported in macropores as a pulse. It is applicable only under the provision that the macropores do not change during the transport of water. The theory cannot be used for modeling water flow in the fissures of shrinking-swelling soils.

In this book, we use the term macropores only for pores without capillarity. In some of the literature a confusion exists inasmuch as coarse capillary pores and by-pass pores are also called macropores just to emphasize the large flux in those pores. However, if capillarity is manifested with the flow realized by the gradient of the negative soil water pressure, the Darcy-Buckingham equation is still appropriate with no need to replace it.

Up to this point we have assumed that the Darcy equation is fully applicable to unsaturated flow. However, when the validity of the Darcy equation is doubted for saturated flow in clays, non-Darcian pre linear flow should be even more pronounced for unsaturated flow in clays. Experiments indicating this possibility (Swarzendruber, 1963) have been theoretically explained (Bolt and Groenevelt, 1969).

The influence of the temperature upon $K(\theta)$ is usually expressed by $\mu_W(T)$ in

$$K(\theta) = K_r(\theta)\, K_p \rho_w g / \mu_w \tag{5.56}$$

However, Constanz (1982) provided experimental evidence that in some instances (5.61) was only approximate.

The influence of the concentration of the soil solution and of the exchangeable cations is similar to that already mentioned for K_S. Dane and Klute (1977) reported that a decrease of the concentration in the soil solution when the SAR was kept constant resulted in roughly the same decrease of K in the whole range of θ, see Fig. 5.13. It is also expected that the function $K(\theta)$ would change with ESP (Kutílek, 1983).

Measuring techniques for determining $K(\theta)$ are usually related to the solution of specified unsteady flow processes, and will be discussed in Chapter 6.

5.3.3 Richard's Equation

Equation (5.32) is fully applicable to steady unsaturated flow when $\nabla \cdot q = 0$, $dq/dt = 0$ and $d\theta/dt = 0$. In practical situations, unsteady flow frequently exists with $d\theta/dt \neq 0$. In these situations, two equations are needed to describe the flux density and the rate of change of θ in time. The flux density is described by the Darcy-Buckingham equation and the rate of filling or emptying of the soil pores is described by the equation of continuity. Consider the prism element having edges of length Δx, Δy and Δz given in Fig. 5.14. The difference between the volume of water flowing into the element and that flowing out of the element is equal to the difference of water content in the element in time Δt. The rate of inflow (macroscopic) in the direction of the x axis is q_x. If we assume the change in q_x is continuous, the rate of outflow is $[q_x + (\partial q_x/\partial x)\Delta x]$. The inflow volume is $q_x \Delta y \Delta z \Delta t$ and the outflow volume is $[q_x + (\partial q_x/\partial x)\Delta x]\Delta y \Delta z \Delta t$. The difference between inflow and outflow volumes is

$$\left\{q_x \Delta y \Delta z \Delta t - \left[q_x + (\partial q_x / \partial x)\Delta x\right]\Delta x \Delta y \Delta z\right\} \tag{5.57}$$

or

$$-\left(\frac{\partial q_x}{\partial x}\right)\Delta x \Delta y \Delta z \Delta t \tag{5.58}$$

Similarly in the direction of the y axis, the difference between the inflow and the outflow volumes is

$$-\left(\frac{\partial q_y}{\partial y}\right)\Delta x \Delta y \Delta z \Delta t \tag{5.59}$$

and that in the direction of the z axis

$$-\left(\frac{\partial q_z}{\partial z}\right)\Delta x \Delta y \Delta z \Delta t \tag{5.60}$$

The sum of the above differences equals the change of the water content of the element. Provided that $q(t)$ has a continuous derivative for $t > 0$,

$$\frac{\Delta\theta}{\Delta t}\Delta x\, \Delta y\, \Delta z\, \Delta t = -\left(\frac{\partial q_x}{\partial x} + \frac{\partial q_y}{\partial y} + \frac{\partial q_z}{\partial z}\right)\Delta x\, \Delta y\, \Delta z\, \Delta t \tag{5.61}$$

Taking the limit as $t \to 0$, we obtain the equation of continuity

$$\frac{\partial\theta}{\partial t} = -\left(\frac{\partial q_x}{\partial x} + \frac{\partial q_y}{\partial y} + \frac{\partial q_z}{\partial z}\right) \tag{5.62}$$

If we insert for q_x, q_y and q_z from (5.32), we have

$$\frac{\partial\theta}{\partial t} = \frac{\partial}{\partial x}\left[K(h)\frac{\partial H}{\partial x}\right] + \frac{\partial}{\partial y}\left[K(h)\frac{\partial H}{\partial y}\right] + \frac{\partial}{\partial z}\left[K(h)\frac{\partial H}{\partial z}\right] \tag{5.63}$$

provided that the soil is isotropic. In one-dimensional form for $H = h + z$ the above equation becomes

$$\frac{\partial\theta}{\partial t} = \frac{\partial}{\partial z}\left[K(h)\frac{\partial h}{\partial z}\right] + \frac{\partial K}{\partial z}. \tag{5.64}$$

Equations (5.63) and (5.64) are called Richard's equations in the name of the author who first derived them (1931).

If the soil is either wetting or drying, θ will be uniquely dependent upon only h and

$$\frac{\partial\theta}{\partial t} = \frac{d\theta}{dh}\frac{\partial h}{\partial t} \tag{5.65}$$

Hence, the capacitance form of Richard's equation is obtained as

$$C_w(h)\frac{\partial h}{\partial t} = \frac{\partial}{\partial z}\left[K(h)\frac{\partial h}{\partial z}\right] + \frac{\partial K}{\partial z} \tag{5.66}$$

5.15

where $C_W = d\theta/dh$ [L^{-1}] is illustrated in Fig. 5.15. An alternative development using

$$\frac{\partial h}{\partial z} = \frac{dh}{d\theta}\frac{\partial\theta}{\partial z} \tag{5.67}$$

leads to the diffusivity form of Richard's equation

$$\frac{\partial\theta}{\partial t} = \frac{\partial}{\partial z}\left[D(\theta)\frac{\partial\theta}{\partial z}\right] + \frac{dK}{d\theta}\frac{\partial\theta}{\partial z} \tag{5.68}$$

where the soil water diffusivity D is the term derived from

$$D(\theta) = K(\theta)\frac{dh}{d\theta}. \tag{5.69}$$

The main reason for the derivation of either the capacitance equation (5.66) or the diffusivity equation (5.68) is the reduction of the number of variables from 4 to 3. Note that the Darcy-Buckingham equation has an the diffusivity form $q = -D(\theta)\frac{\partial\theta}{\partial z} + K(\theta)$ (5.68a)

Both equations (5.66) and (5.68), strongly non-linear owing to functions $C_W(h)$, $K(h)$ and $D(\theta)$, are sometimes called Fokker-Planck equations. The name of (5.68) was derived from its resemblance (when its second term on the right hand side is omitted) to that for molecular diffusion. The units of D in (5.68) are identical to those of the diffusion coefficient. Many analytical and semi-analytical solutions for the diffusivity equation for various boundary conditions are known from the theory of diffusion (Crank, 1956). They have been profitably applied for the solution of many processes of unsaturated flow in soils.

Whenever there is a region of positive pressure in the soil (5.68) is not applicable and (5.66) should be used.

Sometimes, Kirchhoff's transformation

$$U = \int_{h_o}^{h} K(h)\,dh \tag{5.70}$$

is used with (5.64) to yield

$$\frac{C_w(h)}{K(h)}\frac{\partial U}{\partial t} = \frac{\partial^2 U}{\partial z^2} - \frac{1}{K(h)}\frac{dK}{dh}\frac{\partial U}{\partial z} \tag{5.71}$$

or

$$\frac{\partial\theta}{\partial t} = \frac{\partial^2 U}{\partial z^2} - \frac{\partial K}{\partial z}. \tag{5.72}$$

Because the last term of (5.64), (5.66) and (5.68) originated from the gravitational component z of the total potential H, it is frequently referred to as the gravitational term of the Richard's equations. The first term of the right hand side of each of those equations expresses the flow of water in the soil owing to the gradient of the soil water (matric) potential component h. In some instances, the gravitational term is neglected and the non-linear diffusion equation with its non-constant diffusivity

$$\frac{\partial\theta}{\partial t} = \frac{\partial}{\partial z}\left[D(\theta)\frac{\partial\theta}{\partial z}\right] \tag{5.73}$$

is solved approximately. Solutions of the above equation for various boundary conditions are analyzed in the literature dealing with the mathematics of diffusion or heat flow (Crank, 1956, and Carslaw and Jaeger, 1959). If the flow is horizontal, solutions of (5.73) are exact.

5.3.4 Soil Water Diffusivity

5.16

The most common $D(\theta)$ relationship is demonstrated in Fig. 5.16. With the exception of the region of very small soil water contents less than θ_H ($h < -10^5$ cm), the curve steeply rises with θ. Soil water diffusivity $D(\theta)$ in the wet range

above θ_H is typically less steep in its relation to θ as compared with $K(\theta)$. In this range of θ, D changes about five orders of magnitude compared with seven orders of magnitude for K.

In the dry region of $0 \leq \theta < \theta_H$ with a great portion of pores filled with air, water vapor flow is enhanced while liquid water flow is limited to that of very thin water films on the soil solid surfaces. The rate of liquid flow, strongly dependent upon the thickness of the film, has already been demonstrated by (5.36). Here, the vapor flux exceeds the liquid flux. A more detailed discussion on water vapor flux will be given in Section 5.3.5. Now, we shall study in detail the monotonically rising part of $D(\theta)$, i. e. for $\theta > \theta_H$.

Among the well known and frequently used empirical equations is the exponential form (Gardner and Mayhugh, 1958)

$$D = D_o \exp\left[\beta(\theta - \theta_o)\right] \tag{5.74}$$

where D_o corresponds to θ_o and β ranges approximately between 1 and 30. Or,

$$D = \alpha \exp\left[\beta(\theta_E^*)\right] \tag{5.75}$$

where θ_r is replaced by θ_H in θ_E^* and at θ_H, $D = \alpha$. A physically more exact equation should be derived from the soil water retention curve and from $K(\theta)$. Using (4.43) and (5.51) in (5.69), van Genuchten (1980) obtained

$$D(\theta_E) = \frac{K_S(1-m)\theta_E^{1/2-1/m}}{\alpha m(\theta_S - \theta)}\left[\left(1-\theta_E^{1/m}\right)^{-m} + \left(1-\theta_E^{1/m}\right)^{m} - 2\right] \tag{5.76}$$

If the simpler (4.42) is used instead of (4.43) we have

$$D(\theta_E) = \frac{K_S h_A \theta_E^{(b-1)+(a-1)/\lambda}}{\lambda(\theta_S - \theta)} \tag{5.77}$$

with the values of a and b being those given earlier for (5.53) and (5.54).

In some clays, mainly alkali Vertisols, the value of D decreases with an increase of θ, if the soil is confined and not allowed to swell, see Fig. 5.16

(Kutflek, 1984). For some undisturbed soils as well as for disturbed repacked soil columns in the laboratory (Clothier and White, 1981), D does not vary as strongly with θ as discussed above. If $(D_{max} - D_{min})$ is less than one-half an order of magnitude, the linearized form of (5.73)

$$\frac{\partial\theta}{\partial t} = \overline{D}\frac{\partial^2\theta}{\partial x^2} \tag{5.78}$$

serves as an excellent approximation where the mean weighted diffusivity $\overline{D}$ for the wetting process (Crank, 1956) is

$$\overline{D} = \frac{5}{3(\theta_o - \theta_i)^{5/3}}\int_{\theta_i}^{\theta_o}(\theta-\theta_i)^{2/3}D(\theta)d\theta \tag{5.79}$$

and for the drainage process is

$$\overline{D} = \frac{1.85}{(\theta_o - \theta_i)^{1.85}}\int_{\theta_i}^{\theta_o}(\theta-\theta_i)^{0.85}D(\theta)d\theta \tag{5.80}$$

where θ_i is the initial soil water content and θ_o is θ at $x = 0$ for $t > 0$.

Soils manifesting values of D that are constant or nearly so are called "linear soils" because (5.78) is a linear equation. If the Brooks and Corey soil water retention curve (4.42) is used, $K_r(\theta_E)$ is described by (5.53) and $D(\theta_E)$ by (5.77). The condition of a "linear soil" is satisfied if in these equations $[\lambda = -(a-1)/(b-1)]$ or $[a = b = 1]$. If the first condition is applied to the Burdine equation, we obtain $h = h_A\theta_E^2$ and $K_r = \theta_E^{-1}$. Neither of these equations describe physical reality. Similarly, equations of Childs and Collis-George or those of Mualem lead to unacceptable results. The second condition leads to (Kutflek et al., 1985)

$$h = h_A\theta_E^{-1/\lambda} \tag{5.81}$$

$$K_r = \theta_E^{1/\lambda+1} \tag{5.82}$$

and

$$D = -\frac{h_A}{\lambda}\frac{K_S}{(\theta_S - \theta_r)} \tag{5.83}$$

5/32

In general, there exists a family of "linear soils" described by the above equations. If $\lambda = 1$, the hydraulic conductivity function (5.82) is quadratic and meets the requirements of the solutions of Burgers' equation (Clothier et al., 1981).

Concluding, we should keep in mind that the soil water diffusivity is used in Richard's equation in order to reduce the number of variables. It has no direct physical meaning and is only defined mathematically, see (5.69). Moreover, inasmuch as $D(\theta)$ is dependent upon the derivative of the soil water retention curve, it has different values for wetting and drying processes. The temperature dependence of $D(\theta)$ is in accordance with changes of surface tension and viscosity with T. However, its prediction is only approximate owing to some not well understood phenomena that associates the temperature dependence of $h(\theta)$ and $K(\theta)$.

5.3.5 Diffusion of Water Vapor

In section 5.3.4 we have already shown that the relative maximum in the $D(\theta)$ relationship in the dry region is caused by water vapor flow. Indeed, the soil water diffusivity D contains two components: D_L the diffusivity of liquid water, and D_G the diffusivity of water vapor, i. e. the gaseous phase. Hence, $D = D_L + D_G$ (Philip, 1957). Jackson (1964) derived D_G as analogous to the earlier introduced soil water diffusivity

$$D_G = D_p \frac{d\rho_G}{d\theta} \tag{5.84}$$

where ρ_{rG} is the relative density (concentration) of water vapor and D_p the diffusion coefficient of water vapor in soil which is approximated by

$$D_p = D_a \alpha (P - \theta)^{\mu} \tag{5.85}$$

where D_a is the diffusion coefficient of water vapor in free air and α and μ are factors that account for the tortuosity and complexity of the soil porous system. Detailed information about (5.85) is provided by Currie (1961).The term $d\rho_{rG}/d\theta$ is actually the slope of the adsorption isotherm and its inflection point corresponds to the relative maximum of $D_G(\theta)$. The water vapor diffusivity

6/1 Sept, 1993

6 ELEMENTARY SOIL HYDROLOGIC PROCESSES

In this chapter, for the sake of a lucid discussion of soil hydrology, we separate from the global hydrologic cycle those simple elementary processes which take place in the soil. The first group of elementary processes to be discussed are those to be described in the vertical direction and defined by simple boundary conditions. Here we discuss

-infiltration,
-redistribution of water within a soil following infiltration,
-drainage to a water table close to the soil surface,
-evaporation from a bare soil and
-evaporation and transpiration (evapotranspiration) from a soil surface partially vegetated.

Except for infiltration, all the above processes cause a water loss either from the entire soil profile or from at least a particular layer usually from the topsoil when one-dimensional vertical flow is assumed. When two- and three-dimensional flow is considered owing to field circumstances, lateral subsurface and hypodermic flows may contribute to the water balance within the soil profile.

Meteorological situations actually control the extent of the elementary processes, and together with the water storage capacity of the soil profile, a particular stage of a hydrologic regime evolves over a long time period. If these stages are combined and averaged over still a longer span of time, we speak of a hydrologic regime of a soil. Analogously, as meteorological situations refer to weather during a period of weeks or months in a particular area, combined, long time averages are considered as the climate of the area.

6.1 PRINCIPLES OF SOLUTIONS

Our knowledge of elementary soil hydrologic processes stems partly from properly performed experiments and partly from mathematical solutions of equations describing physical processes. In each of the procedures we simulate the process either physically by an experiment or mathematically using either analytical or numerical methods. When we speak of properly performed

experiments, we must experimentally impose exactly the initial and boundary conditions. Before imposing the boundary conditions, we first establish the initial conditions - the values of θ or h at all z of the one-dimensional column at $t < 0$. When the initial condition demands a zero flux ($q = 0$), it is imperative that $dH/dz = 0$ along the entire column. When the initial value of the soil water content θ_i is assumed constant with depth ($d\theta_i/dz = 0$), a flux corresponding to a unit gradient of H exists, i. e. $q = -K(\theta_i)$ provided that a continuity of liquid water exists. If θ_i is very small, the downward flux may be negligibly small. Altering the value of the variable θ or h, respectively, at the boundary (i. e. at the topographical soil surface) induces a non-equilibrium condition that generates a soil water flux within the soil profile. Non-steady fluxes will then persist in the system until an equilibrium is reached with $q = 0$, or until the flux is invariant with time ($dq/dt = 0$) and a steady state flux density is reached. Another possibility for causing water flow in soil is by imposing a defined flux density $q(t)$ on the boundary $q_o(t)$.

One boundary of a one-dimensional soil column is its topographical surface. The other boundary is that of a column having either a finite or infinite length. A finite column is used to manifest a field condition, e. g. a ground water table ($h = 0$) or a defined water content or water flux at its bottom end. If the column extends to infinity, we speak of a semi-infinite column with its lower boundary $z \rightarrow \infty$.

If we establish a new value of the variable θ or h on a boundary for $t \geq 0$, we obtain Dirichlet's (or a concentration) boundary condition (DBC). When a flux density is imposed for $t \geq 0$ on a boundary, we have Neuman's (or a flux) boundary condition (NBC). If θ or h is specified on one boundary and a flux is specified on the other boundary, we have a mixed boundary condition (MBC).

When we solve a steady flow problem which is characterized by $dq/dt = 0$ and $dq/dz = 0$, we do not define the initial condition because the flux and variables θ and h are independent of time. The solution is a particular value of the flux q for which a unique distribution of θ and h, respectively, along the z axis exists.

Distributions of non-steady flow problems yield distributions of θ or h, respectively in space and time. These distributions $\theta(z, t)$ and $h(z, t)$ for one-

dimensional problems are usually given as continuous functions $\theta(z)$ or $h(z)$ for specific times or time intervals. For DBC we are frequently searching additionally for the flux density at the boundary $q_o(t)$. In an experiment we must establish the initial θ_i or h_i at all depths for $t < 0$ and sustain θ_o or q_o at the boundary during the entire experiment. It is imperative that the experimental initial and boundary conditions are matched exactly with those described mathematically. Without such initial and boundary conditions, the experimental results cannot be properly evaluated and generalized.

In the mathematical treatment of problems, the initial and boundary conditions represent the limits of integration. Additionally, the properties of the soil need to be characterized. When we describe the process mathematically, we characterize the soil by its hydraulic characteristic functions K_S, θ_S, $h(\theta)$ and $K(\theta)$ or $K(h)$. $D(\theta)$ is obtained from $K(\theta)$ and $h(\theta)$ or is defined directly from primary measurements. Methods for obtaining the hydraulic functions will be discussed later in Chapter 7

Mathematical solutions of the elementary hydrologic processes are either analytical or numerical. In *analytical procedures* , differential equations are usually integrated only after some kind of transformation. Many analytical procedures exist for somewhat trivial boundary conditions of unsteady flow in soils defined by simple hydraulic functions and for steady flow processes in homogeneous or distinctly layered soil columns. The analytical solutions typically involve infinite series or transcendental functions that are evaluated by numerical methods with the assistance of a computer. As a result, the calculated results are approximate in spite of having an exact analytical solution.

Close to analytical solutions are the *quasi-analytical solutions* for which a significant part of the procedure involves an analytical procedure. The overall equation, often reduced to one or more ordinary differential equations, is integrated using a convergent iterative scheme. Alternatively, we split the higher order partial differential equation (e. g. Richard's equation) into lower order differential equations that are solved separately. In such cases an auxiliary function is frequently assumed with its value being determined by consecutive iterations. Analytical and quasi-analytical solutions developed for some elementary soil hydrological processes fit soils with simple, special forms of

hydraulic functions. Such solutions, even if they are not directly applicable to field situations, have a great advantage. They lead to a full understanding of the physical process and provide estimates of deviations, e. g. owing to an alteration of a boundary condition. Moreover, these solutions allow errors of estimation of approximate and numerical procedures to be quantified. *Approximate solutions* are frequently exact analytical solutions developed for a soil process characterized by a simple or even oversimplified hydraulic function. Or, they are exact solutions for a very simple flow process that only approximates reality in the field.

Numerical methods used in the solution of soil hydrologic processes are procedures which enable us to replace a differential equation with a set of approximate algebraic equations solved with a computer. These approximate numerical procedures are (i) the method of finite differences and (ii) the method of finite elements. Although their theoretical derivations are based upon different mathematical approaches, there are many similarities between both methods.

In the method of finite differences the spatial domain within which we search for a solution is sectioned by a system of normals into small segments. In 1-dimensional problems we obtain line segments, in 2-dimensional problems rectangle segments and in 3-dimensional problems parallelepiped segments. For each node of these geometric segments, we determine the value of the differential function describing the problem.

We replace the derivatives at a point by differences of the variable over a small finite interval. This method for the function $h(z)$ is therefore the inverse of the definition of its derivative

$$\frac{dh}{dz} = \lim_{\Delta z \to 0} \frac{h(z+\Delta z) - h(z)}{\Delta z} \qquad (6.1)$$

Inasmuch as the approximation at one point depends to a certain degree upon approximations at neighboring points, local approximations are controlled by approximations applicable to the entire domain.

The continuous analytical equation is replaced by a set of algebraic equations with differences substituting for derivatives of functions obtained from Taylor's series expansions.

In finite element methods, the domain of the solution is subdivided into n smaller sub domains, i. e. finite elements. The simplest scheme is composed of triangles with a triangular pyramid erected over each node. The value of the base functions represents the approximate solution with time taken as the finite difference. Local approximation is the characteristic feature of the finite difference method. In contrast, the finite element method manifests a global view. Assuming that the solution is expressible by a set of basic functions, the most frequent procedures are those of Galerkin and Ritz which are both based upon minimizing a quadratic function.

For a full appreciation of numerical methods, the reader should study fundamental and applied concepts provided in the literature (e. g. Remson et al., 1971, Neuman, 1975; Pinder and Gray, 1977 and Vauclin et al., 1979).

Numerical methods offer *ad hoc* solutions which are successful for non-trivial boundary conditions and for soils having hydraulic functions not described by simple functions. Additionally, they can be advantageously used to study water flow in heterogeneous soils. Numerical methods offer a large number of solutions for studying soil parameters under a wide range of conditions. They may in some instances replace results of experimental studies which are difficult to carry out owing to (i) slowly changing conditions over excessively long time periods, (ii) excessive number of experiments needed for alternative initial and boundary conditions and (iii) some of the acting factors for some problems may not be experimentally separated and uniquely studied.

In spite of all their advantages, numerical studies cannot generally substitute for analytical solutions and experiments. Analytical methods are useful to test the validity of numerical procedures adopted as standard solutions, and they are particularly helpful to establish the behavior of solutions in the neighborhood of singularities. Experimental observations compared with numerical simulations demonstrate how well our simplified formulations capture the essence of complex, natural soil processes.

6.2 INFILTRATION

The term infiltration denotes the entry of water into the soil through its surface. The soil surface could be plane, concave or convex, and could be formed by the walls of a cavity of a defined shape such as a sphere, cylinder etc. The source of water can completely or only partially cover the entire surface. Equations describing infiltration are usually for 1-dimensional water flow in either the vertical or horizontal direction. A limited number of solutions exist for 2- and 3-dimensional infiltration processes. Here, we restrict our discussion to 1-dimensional, vertical infiltration. Implicitly, our solutions are valid for infiltration through a plane horizontal surface.

Hydrologically, the infiltration process separates rain into two parts. One part stored within the soil supplies water to the roots of vegetation and recharges ground water. The other part which does not penetrate the soil surface is responsible for surface runoff. Infiltration is therefore a pivotal point within the hydrologic cycle.

Being consistent with present-day terminology, we shall call the flux density of water across a topographical soil surface the infiltration rate. However, this infiltration rate is often confusingly described by terms such as infiltration velocity, infiltration capacity, infiltrability etc. in relation to a specifically imposed boundary condition and in accordance with only some kind of subjective criteria. For non-steady flows it is clear that the flux density is time dependent and moreover, when boundary conditions are changed, the flux density responds and is also time dependent. Thus, we could formulate a voluminous number of terms describing still the same phenomenon - the flux density across the top boundary of the soil.

We shall discuss separately steady and unsteady infiltration owing to the different hydraulic characteristics of both flows. Although steady infiltration is simpler to solve and to understand because only the Darcy-Buckingham equation is involved, unsteady infiltration is the dominant process in nature. We shall discuss unsteady infiltration in two sections according to the boundary conditions governing the type of infiltration. When the soil surface is

instantaneously and excessively ponded as it is in an infiltration test performed with a ring infiltrometer, we have Dirichlet's boundary condition (DBC). When infiltration occurs under natural rainfall, we meet Neuman's boundary condition (NBC) for the full duration of the rain or for at least its initial occurrence. With these two types of flow being fundamentally different, we shall consider them separately.

6.2.1 Steady Infiltration

Steady infiltration is characterized by the condition that the flux density does not change with time nor with position in the unsaturated soil, i. e. $\partial q/\partial t = 0$ and $\partial q/\partial z = 0$. It follows from the equation of continuity (5.62) repeated here for 1-dimension

$$\frac{\partial \theta}{\partial t} = -\frac{\partial q}{\partial z} \tag{6.2}$$

that the soil water content does not change in time (i. e. $\partial\theta/\partial t = 0$ as well as $\partial h/\partial t = 0$). In order to satisfy the condition $\partial h/\partial t = 0$, we must define a non-variant hydraulic condition at the bottom of the soil column. The simplest practical provision is a constant ground water level at its bottom. Such conditions are simply demonstrated by the following process. A rain intensity q_R is constant in time ($\partial q_R/\partial t = 0$) and equals the infiltration rate as well as the flux density in the soil q provided that $q_R < K_S$. In this case, rainfall has been constant and infiltration has lasted long enough to allow the wetting front to reach the ground water level. We further assume that the ground water level is kept at a constant elevation by e. g. a drainage system. It is mathematically convenient to identify the origin of the z coordinate at the ground water level from which z increases positively upwards. As a result at $z = 0$, $h = 0$ and at the soil surface $z = Z$, $h = h_Z$ and $q = -q_R$. Some solutions derived for steady state conditions approximate non-steady infiltration after a long time has elapsed when $\partial q/\partial t \rightarrow 0$. For example, the development of a $h(z)$ or $\theta(z)$ profile in a crust-topped soil or in a soil with distinct horizons of different hydraulic functions and conductivities is practically identical for either steady state infiltration or the quasi-steady stage of non-steady infiltration after a long time.

6.2.1.1 Homogeneous Soil Profile

(6.1)

Here, inasmuch as the direction of flow is oriented downward while the positive direction of the z-axis is upward, the flux density $q < 0$. Equation (5.34) repeated here is

$$q = -K(h)\frac{dH}{dz} \tag{6.3}$$

where $H = (h + z)$. We obtain $q < 0$ when $dH/dz > 0$. If indeed, $dH/dz = 0$, we have a state of equilibrium with $q = 0$ and $h = -z$. The domain of $h(z)$ which satisfies (6.3) is therefore limited from the left side of the graph in Fig. 6.1 by $h = -z$ ($q = 0$) and from the right side of the domain by $q = -K_S$ with $dH/dz = 1$ and $dh/dz = 0$. For the determination of $h(z)$ we integrate (6.3) with an appropriate expression for $K(h)$. For an exponential expression of $K(h)$, see (5.39)

$$K = K_S \exp(ch)$$

we obtain for the limit $h = 0$ at $z = 0$

$$\int_0^z dz = -\int_0^h \frac{K_S\, dh}{q\exp(-ch) + K_S} \tag{6.4}$$

After integration we have

$$z = \frac{1}{c}\ln\left[\frac{q + K_S}{q + K_S\exp(ch)}\right] \tag{6.5}$$

(6.2)

Solution (6.5) is represented graphically in Fig. 6.2. For measured values of K_S and c, we obtain values of z for a series of selected values of h using the appropriate values of K_S/q. We obtain $\theta(z)$ shown in Fig. 6.1 using the soil water retention curve SWRC. We see in the left graph that the depth of the zone having $dh/dz = 0$ increases with increasing absolute magnitudes of q. Also, within this zone $q = -K$ and $d\theta/dz = 0$. For example, for $q = -0.4$ cm/h, (h, θ) at z = 300 and 500 cm are (-79.98, 0.3396) and (-80.46, 0.3387), respectively, see the right hand graph. Hence, if we measure h or θ for a series of steady-state infiltration

fluxes q_n into a homogeneous soil with a water table at great depth, we obtain $K_n(h) = |q_n|$ or $K_n(\theta) = |q_n|$, respectively.

An equation similar to (6.5) is easily derived for a soil manifesting an air entry value h_A when a $K(h)$ function described by (5.40) is used in (6.3). Soil water pressure head profiles calculated for $h_A = -20$ cm are shown in Fig. 6.3 for some values of q_n given in Fig. 6.1. Note that the height of the water-saturated zone above the ground water level is not constant but rises with an increase of $|q|$. And, if $q = 0$, the height of the saturated zone above the ground water level reaches only its minimum value, $z = -h_A$, see Fig. 6.3. Such observations are a graphical illustration that hydrostatic conditions differ markedly from those involving systems where water is flowing.

(6.3)

Many additional solutions of infiltration for other expressions of $K(h)$ have been reported by Kutílek (1984).

6.2.1.2 Layered Soil Profiles

The simplest case is the crust-topped profile. Rainfall frequently destroys soil aggregates within a soil surface. Or, if infiltration lasts for a long time, the source of water is often from a river or waste discharge carrying suspensions of clay or fine particles which are deposited on the soil surface or within the soil profile. Each of those processes denoted by sealing, crusting, collimation etc. results in the formation of a less permeable soil surface layer. Here for the sake of simplicity, we shall use the term crust for the result of all such processes. The characteristics of the crust will be denoted by the index 2, while those of the soil below the crust will be given the index 1, see Fig. 6.4. The origin of the z-axis is again identical with the position of the ground water level which is kept constant. The thickness of the soil between the ground water level and the crust is L_1, the thickness of the crust L_2 and the depth of water on the soil surface h_o. For steady-state flow, $q_1 = q_2$, and we have

(6.4)

$$K_1\left(\frac{dH}{dz}\right)_1 = K_2\left(\frac{dH}{dz}\right)_2 \tag{6.6}$$

If $K_{S1} \gg K_{S2}$, and $K_1(h_I) \gg K_2(h_I)$ where h_I is the value of h at the interface, we have

$$\left(\frac{dH}{dz}\right)_1 << \left(\frac{dH}{dz}\right)_2 \qquad (6.7)$$

and because $H = (h + z)$,

$$\left(\frac{dh}{dz}\right)_1 << \left(\frac{dh}{dz}\right)_2 \qquad (6.8)$$

This condition of a larger gradient of h occurring in the crust (layer 2) demands a sufficiently small value of h_I including $h_I < 0$. Because we assume that just below the interface in the subsoil (layer 1), $dH/dz \approx 1$, we can write

$$q = - K_1(h_I). \qquad (6.9)$$

For the crust assuming it remains water-saturated,

$$q = - K_{S2}\left(\frac{h_o + h_I + L_2}{L_2}\right) \qquad (6.10)$$

We also assume here that $h_{A2} = 0$ and $h_{A1} = 0$. The value of h_I is obtained by equating (6.9) and (6.10).

The criterion for $h_I < 0$ is derived from the total head loss between the free water level on the soil surface and that of the ground water - $(h_o + L_1 + L_2)$. Inserting this head loss into the modified Darcy equation (5.10) with the hydraulic resistance R_i for each of the two layers, we obtain

$$q = - \left(\frac{h_o + h_I + L_2}{R_1 + R_2}\right) \qquad (6.11)$$

The soil below the crust will be unsaturated if $|q| < K_{S1}$. From (6.11) it can be shown that the condition for unsaturation below the crust is

$$h_o < L_2\left(\frac{K_{S1}}{K_{S2}} - 1\right) \qquad (6.12)$$

if $h_{A1} = 0$. Because $L_2 \neq 0$, unsaturated flow below the crust exists anytime the soil is ponded with water provided $h_{A1} = 0$. The unsaturated condition (6.12) is also valid for $h_{A2} < h_I$. For $h_{A2} > h_I$, the bottom part of the crust is also unsaturated, and $h(z)$ has a curved shape, see (b) in Fig. 6.4. For such cases, the above approach has to be modified, see e. g. Takagi (1960), Srinilta et al. (1966) and Bear et al. (1968). Kutflek (1984) provides additional solutions when $dH/dz < 1$ below the interface.

Once $h(z)$ is known, we can determine $\theta(z)$ in the entire profile. Although h(z) has to be continuous, $\theta(z)$ is frequently discontinuous at the interface, see Fig. 6.4. When criterion (6.12) is fulfilled, the soil below the crust will be unsaturated if $h_{A1} > h_I$ provided the SWRC manifests h_A.

If a soil profile has n layers (or horizons) with each layer having its unique value of K_S and $K(h)$, we integrate in intervals identical with the height of the layers z_n. As a practical example, let us assume that the soil profile consists of 5 layers, see Fig. 6.5. The sequence of numbers again follows the positive direction of the z-axis with the layer in contact with the ground water level being 1, the next higher being 2 etc. Let us suppose that the soil has a strongly developed Bt horizon with a very small hydraulic conductivity, our layer 3. If $|q| > K_{S3}$ then for layer 3 we find that $(dH/dz)_3 > 1$, or $(dh/dz)_3 > 0$. For the other layers $dH/dz \leq 1$ and $dh/dz \leq 0$, see Fig. 6.5. The distribution $h(z)$ can be found either analytically or with the graph in Fig. 6.2. We start with layer 1 as if it were a homogeneous profile to obtain h_1 on the boundary between layers 1 and 2. For layer 2 we find what would be the position of the ground water level to obtain h_1 for the given value of q. Let us call this position ξ_2 a substitute ground water level for soil layer 2, see Fig. 6.5. With ξ_2 we determine $h(z)$ between z_1 ad z_2, and at z_2, $h = h_2$. In layer 3 which has the very small hydraulic conductivity, we assume $h_2 \geq h_{A3}$ and $h(z)$ is linear. If indeed $h_2 < h_{A3}$, we proceed analytically to obtain the distribution $h(z)$, see Kutflek (1984). Or, alternatively, we approximate reality by a linear relation as we did for $h_2 > h_{A3}$. Note that a linear increase of h for the sub layer with $h > h_A$ or for $h > 0$ is exact. Having obtained the valu· of

6.5

h_3, we use in layer 4 Darcy's equation for the saturated flow which occurs in the domain $h \geq h_{A3}$. From the elevation z where $h = 0$, we follow the same procedure as that already described for a simple 2-layer soil profile.

It follows from the above analysis that the less permeable layer in a profile acts as a hydraulic resistance which causes the development of a saturated zone in and above this layer provided that the flux density is greater than K_S of this less permeable layer. The thickness of the saturated zone increases with q, or for a given q, it increases with a decrease of K_S in the less permeable layer.

In Fig. 6.5, the zone of saturation starts above the top boundary of the less permeable layer 3 and ends above the bottom boundary of layer 3 provided that $h_{A3} = 0$. For $h_{A3} \neq 0$ the thickness of the saturated zone is greater.

The example described above also explains the conditions for a pseudo-gley formation in layers 3 and 4 during long term steady rainfall, even without the presence of a water table.

6.2.2 Unsteady Infiltration, Dirichlet's Boundary Condition (DBC)

Assuming that a soil surface is continuously flooded with a negligibly small depth of water at time $t \geq 0$, the surface soil will be water-saturated. Before the soil surface is flooded ($t \leq 0$), we assume that the initial soil water content $\theta = \theta_i$. Water supplied to the surface keeps the surface soil at saturation ($\theta = \theta_S$) but is never allowed to rise significantly above the soil surface.

Such a situation defines Dirichlet's boundary condition (DBC) for infiltration into a semi-infinite homogeneous soil. With z increasing positively downward and $z = 0$ identified at the soil surface, the DBC is

$$t \geq 0 \qquad z = 0 \qquad \theta = \theta_S, \tag{6.13}$$

$$t \geq 0 \qquad z = 0 \qquad h = h_o, \tag{6.14a}$$

or

$$t \geq 0 \qquad z = 0 \qquad h = 0. \tag{6.14b}$$

We use (6.13) when the diffusivity form of the Richard's equation (5.68) is solved and (6.14) for the capacitance form (5.66). Less frequently, the time dependent behavior of $\theta(t)$ or $h(t)$ are defined at the soil surface.

The initial condition for the simplest case is

$$t = 0 \qquad z > 0 \qquad \theta = \theta_i \tag{6.15}$$

Initial conditions were discussed in detail at the beginning of section 6.1. The initial condition is sometimes considered as a boundary condition with $t = 0$ taken as a boundary similarly to $z = 0$.

Boundary condition (6.14a) has the advantage that it specifies the depth of water flooding the surface, i. e. the pressure head on the surface. Flooded alluvium along a river, flooded infiltration in an irrigation basin or in a basin for tertiary sewage treatment are practical examples of that boundary condition. Or, late periods of some rainfall events are other examples of (6.13). If a basin is flooded at $t = 0$ without additional water being provided, the decreasing level of water in the basin equals the cumulative infiltration I. Inasmuch as I is a function of t, we have for the DBC at $z = 0$, $h(t) = [h_o - I(t)]$ where $h = h_o$ at $t = 0$.

6.6

Infiltration caused by a DBC is frequently demonstrated with data from infiltration tests using double ring infiltrometers. The infiltration rate is measured by observing the decreasing water level within the inner ring, or even better, by measuring the inflow provided from a mariotte flask to the ring in order to keep a constant water level. The outer ring serves as a hydraulic buffer zone to minimize lateral flow below the inner ring. As a result, flow paths below the inner ring are nearly vertical, see Fig. 6.6. However, because a slight divergence of flow paths in the inner ring cannot be avoided, the measured data do not represent exactly 1-dimensional infiltration. Generally, the error is negligible compared with the inaccuracy of field experimentation and the spatial and temporal variability of the soil hydraulic functions provided that the soil is vertically homogeneous.

When distinct soil layers exist in a profile, a strong divergence of flow paths occurs and the assumption regarding 1-dimensionality of the experiment is violated, see Fig. 6.6c. Hence, the measured data can be evaluated only for the period up to the time when the wetting front reaches the top boundary of the lesser permeable layer.

6.2.2.1 Characteristics of Infiltration

The primary data are measured values of cumulative infiltration I expressed as [L], usually in cm as a function of time. The values represent the total amount of water infiltrated into the soil surface from the beginning of the infiltration test at $t = 0$. A typical $I(t)$ relationship is a smooth, monotonically rising curve, see Fig. 6.7. The infiltration rate $q_o = -dI/dt$ where the subscript o refers to the soil surface at $z = 0$. The value of $|q_o|$ initially decreases rapidly with time and eventually approaches a constant value. For $t = 0$, $|q_o| \rightarrow \infty$, and for $t \rightarrow \infty$, $q_o =$ constant. Theoretically, $|q_o| \rightarrow K_S$ as $t \rightarrow \infty$, see Fig. 6.7. Practically, the infiltration rate starts to be constant for coarse textured soils only after decades of minutes while that for fine textured loams is in the order of hours, depending upon the hydraulic functions of the soil and θ_i. Infiltration sometimes denoted as quasi-steady after this time limit will be discussed more fully in section 6.2.2.2. Steady infiltration into a crust-topped profile or into a layered profile can be successfully analyzed when 1-dimensional flow is guaranteed, e. g. by ponding water on a large area at $t = 0$ when the ground water level is at great depth or absent. The shape of $q_o(t)$ is empirically approximated by either a hyperbolic or exponential curve.

(6.7)

(6.8)

For a solution of the infiltration problem we first search for $h(z, t)$ and from it we obtain $\theta(z, t)$ from the SWRC. Some solutions provide $\theta(z, t)$ directly. Two examples of $\theta(z, t)$, one for sand and one for light clay are given in Fig. 6.8. The profiles are "piston-like", particularly for the sand. Where θ decreases steeply with z is called the wetting front. The rate of progress of the wetting front into the sand profile is more than two orders of magnitude greater than that into the clay profile. As the depth of wetting increases the shape of the wetting front becomes more gradual, especially for the clay. As infiltration proceeds, the shapes of $\theta(z)$ profiles for a given soil become nearly identical. Theoretically, the shapes are identical as $t \rightarrow \infty$.

Integration of the soil moisture profile at time t defines the cumulative infiltration at time

$$I = \int_{\theta_i}^{\theta_s} z \, d\theta \tag{6.16}$$

which according to (6.15) will decrease as θ_i increases. The influence of the initial value of water content θ_i is demonstrated in Fig. 6.9 for the light clay. If $\theta_i / \theta_S \geq 0.95$, the infiltration rate q_o can be approximated by $|q_o| \approx K_S$. The influence of the depth of ponding on the soil surface upon $q_o(t)$ is illustrated in Fig. 6.9. For $0 \leq h_o \leq 2$ cm, the influence is negligibly small. For $h_o = 10$ cm, the value of $|q_o|$ is increased by 20% for large times and by more than 50% for short times. These relationships demonstrate how important it is to keep the value of h_o constant and as small as possible in experiments when the DBC (6.13) is applied.

(6.9)

Solutions to this type of infiltration can be divided into the three classes - (i) analytical and semi-analytical procedures, (ii) approximate solutions and (iii) empirical equations.

6.2.2.2 Analytical and Semi-Analytical Procedures

Richard's equation in its diffusivity form (5.68) is repeated here for the vertical coordinate oriented positively downward from the soil surface located at $z = 0$

$$\frac{\partial \theta}{\partial t} = \frac{\partial}{\partial z}\left[D(\theta) \frac{\partial \theta}{\partial z} \right] - \frac{dK}{d\theta} \frac{\partial \theta}{\partial z} \tag{6.17}$$

This equation, sometimes denoted as the non-linear Fokker-Planck equation (Philip, 1969), is non-linear owing to the strong dependence of D and K upon θ. The first term on the right-hand-side of (6.17) describes the transport of water owing to the initial degree of unsaturation of the soil profile. Therefore, as θ_i increases, the importance of this term decreases. The second term on the right-hand-side of (6.17) originates because the gravitational potential. Hence, it is

called the gravitational term and describes the flow of water owing to the force of gravity.

Philip's (1957) solution of (6.17) is based upon the idea of separating the infiltration into its two components - those caused by the matric potential force and by the gravitational potential force. The idea is illustrated in Fig. 6.10. In the first step, he neglected the gravitational force and obtained a solution for horizontal infiltration in the form $x(\theta, t)$. Here, the dependent variable was changed to that of the horizontal axis x. Next, he assumed that the real $z(\theta, t)$ for vertical infiltration was the horizontal component $x(\theta, t)$ plus a correction , see Fig. 6.10. The correction owing to the gravitational force is time dependent. The influence of gravity upon infiltration is shown in Fig. 6.10 when θ_i is small. For short infiltration times its influence is very small, but with time it increases and for very large times, the force of gravity dominates the process. Hence, we first study horizontal infiltration.

6.10

Our horizontal soil column, initially at an unsaturated water content θ_i, has its end at $x = 0$ maintained at water saturation θ_S. Hence, for

$$t \geq 0 \qquad x = 0 \qquad \theta = \theta_S \tag{6.18}$$

$$t = 0 \qquad x > 0 \qquad \theta = \theta_i \tag{6.19}$$

we solve (6.17) without the gravitational term

$$\frac{\partial \theta}{\partial t} = \frac{\partial}{\partial x}\left[D(\theta)\frac{\partial \theta}{\partial x}\right] \tag{6.20}$$

It is only here for a homogeneous soil (i. e. not layered) that the gradient of θ represents the driving force of the process. When D is a constant in (6.20), the solution is according to Carslaw and Jaeger (1959)

$$\frac{\theta - \theta_i}{\theta_s - \theta_i} = erfc\left(\frac{x}{2\sqrt{Dt}}\right) \tag{6.21}$$

When D is a function of θ, we transform (6.20) into an ordinary differential equation using the Boltzmann transformation. The transformed equation has a new variable η instead of the two original variables x and t. The new variable η defined by the Boltzmann transformation

$$\eta(\theta) = x t^{-1/2} \tag{6.22}$$

leads to

$$\frac{\partial \eta}{\partial t} = -\frac{1}{2} x t^{-3/2} = -\frac{\eta}{2t} \tag{6.23}$$

$$\frac{\partial \theta}{\partial t} = \frac{d\theta}{d\eta}\frac{\partial \eta}{\partial t} = -\frac{\eta}{2t}\frac{d\theta}{d\eta} \tag{6.24}$$

$$\frac{\partial \eta}{\partial x} = t^{-1/2} \tag{6.25}$$

and

$$\begin{aligned}\frac{\partial}{\partial x}\left[D(\theta)\frac{\partial \theta}{\partial x}\right] &= \frac{\partial}{\partial \eta}\left[D(\theta)\frac{d\theta}{d\eta}\frac{\partial \eta}{\partial x}\right]\frac{\partial \eta}{\partial x} \\ &= \frac{\partial}{\partial \eta}\left[D(\theta)\frac{d\theta}{d\eta}t^{-1/2}\right]t^{-1/2}\end{aligned} \tag{6.26}$$

From the above (6.20) transforms to

$$-\frac{\eta}{2}\frac{d\theta}{d\eta} = \frac{\partial}{\partial \eta}\left[D(\theta)\frac{d\theta}{d\eta}\right] \tag{6.27}$$

The transformed boundary conditions are

$$\eta = 0 \qquad \theta = \theta_S \tag{6.28}$$

$$\eta = \infty \qquad \theta = \theta_i \tag{6.29}$$

6.11

The solution for which we search is simply $\theta(\eta)$, see Fig. 6.11. Measured soil water profiles $\theta[x(t_1)]$, $\theta[x(t_2)]$, $\theta[x(t_3)]$ etc. are thus transformed into the unique $\theta(\eta)$ relationship by merely dividing x by $t_1^{1/2}$ for the first profile, $t_2^{1/2}$, for the second profile etc. Note that for $t = 1$, $x \equiv \eta$. Hence, the physical reality of $\theta(\eta)$ is the soil water profile $\theta(x)$ when the infiltration time is unity.

Philip (1960) and Kutflek (1984) have shown for which analytical expressions of $D(\theta)$ analytical solutions of (6.27) subject to (6.28) and (6.29) exist. Because it is exceptional that any of those analytical expressions accurately describe $D(\theta)$ of a real soil, an iterative procédure proposed by Philip (1955) is commonly used to calculate $\theta(\eta)$ from measured distributions of D versus θ.

With the content of infiltrated water being denoted as cumulative infiltration I,

$$I = \int_{\theta_i}^{\theta_s} x \, d\theta \tag{6.30}$$

or with (6.28),

$$I = \int_{\theta_i}^{\theta_s} \eta(\theta) \, t^{1/2} \, d\theta \tag{6.31}$$

Inasmuch as $\eta(\theta)$ is unique for each soil, Philip (1957) introduced the term sorptivity S [$LT^{-1/2}$]

$$S = \int_{\theta_i}^{\theta_s} \eta(\theta) \, d\theta \tag{6.32}$$

and

$$I = S \, t^{1/2} \tag{6.33}$$

Because the infiltration rate

$$q_o = dI / dt, \tag{6.34}$$

we have

$$q_o = \frac{1}{2} S \, t^{-1/2} \tag{6.35}$$

6.12

Here, we note that the sorptivity is physically the cumulative amount of water infiltrated at $t = 1$, and at that time, the infiltration rate has diminished to one-half the value of S. Sorptivity depends not only upon the $D(\theta)$ function but upon θ_i. The value of S decreases with increasing θ_i and as $\theta_i \to \theta_S$, $S \to 0$, see Fig. 6.12. When S is measured for a particular θ_{i1}, we can linearly interpolate between θ_{i1} and θ_S in order to obtain a first approximation of S for $\theta_{i2} > \theta_{i1}$. A more laborious, exact procedure is described by White and Broadbridge (1989). If $\theta_o < \theta_S$ is used in (6.18) instead of θ_S, we proceed in the same manner to derive S. However, the resulting value of $S(\theta_i, \theta_o)$ may indeed drop substantially from that of $S(\theta_i, \theta_S)$.

Sorptivity is an integral part of most investigations describing vertical infiltration. As a first approximation of the solution of (6.17) subject to (6.18) and (6.19), Philip used (6.20), the solution of (6.21) for horizontal infiltration, i. e. $z_1(\theta, t) = x(\theta, t)$. He corrected this approximation with the term y, i. e. $z = z_1 + y$. However, because an exact value of y cannot be obtained, its approximation y_1 defines another correction u, i. e. $y = y_1 + u$. Again, instead of an exact u we can only find still another estimate u_1 etc. Hence, Philip obtained the infinite series solution

$$z(\theta, t) = \eta_1(\theta) t^{1/2} + \eta_2(\theta) t + \eta_3(\theta) t^{3/2} + \cdots + \eta_n(\theta) t^{n/2} \tag{6.36}$$

where the functions $\eta_1, \eta_2, \eta_3, \cdots \eta_n$ are defined with $D(\theta)$, $K(\theta)$ and η_{n-1}. The procedure for computing terms η_n is described in detail by Kirkham and Powers (1972).

Inasmuch as the cumulative infiltration I according to (6.16) is

$$I = \int_{\theta_i}^{\theta_s} z \, d\theta \, . \tag{6.37}$$

Philip formulated analogously to the sorptivity equation (6.32) for horizontal infiltration, the following equation from (6.36)

$$I = S t^{1/2} + \left(A_2 + K_i\right)t + A_3 t^{3/2} + \cdots + A_n t^{n/2} \qquad (6.38)$$

where

$$A_n = \int_{\theta_i}^{\theta_s} \eta_n(\theta)\, d\theta \qquad n = 2, 3, \cdots$$

and K_i is $K(\theta_i)$. Note that $K_i t$ expresses the cumulative water flow with $dH/dz = -1$ at $\theta = \theta_i$. Thus, we understand physically that boundary condition (6.19) can be kept only if we impose a steady flux density $q_o = K(\theta_i)$ for $z \geq 0$ within the semi-infinite column.

The series (6.38) converges for short and intermediate times of infiltration and the infiltration rate $q_o(t)$ obtained by differentiation is

$$q_o = \frac{1}{2} S t^{-1/2} + \left(A_2 + K_i\right) + \frac{3}{2} A_3 t^{1/2} + \cdots + \frac{n}{2} A_n t^{n/2-1} \qquad (6.39)$$

For large times, (6.38) does not converge. Inasmuch as the shape of the wetting front remains invariant at large times, the wetting front moves downward at a rate

$$v = \left(\frac{K_s - K_i}{\theta_s - \theta_i}\right) \qquad (6.40)$$

while the infiltration rate for $t \to \infty$ is

$$q_o = K_s . \qquad (6.41)$$

Equations (6.40) and (6.41), commonly called the infinite time solutions, are theoretically traveling wave solutions (Philip, 1969).

The times for which (6.38) or (6.39) continue to converge was found to range broadly from 0.67 h for sand to 250 h for light clay (Haverkamp et al., 1988). Similarly, the times for which the infinite time solution is applicable varies widely from approximately 100 min for a silt loam (Nielsen et al., 1961) to about 10^5 min for light clay (Kunze and Nielsen, 1982). Piece wise solutions for 1-dimensional infiltration have been discussed by Philip (1987).

In order to obtain an intermediate time solution, Swartzendruber (1987) adjusted Philip's time series solution of q to apply between the limits $t \to 0$ and $t \to \infty$. Inasmuch as the solution for infiltration into linear soils as well as some approximate solutions lead to exponential forms of $I(t)$, Swartzendruber proposed intuitively the form

$$I = \frac{S}{A_o}\left[1 - \exp\left(-A_o t^{1/2} - B_o t - C_o t^{3/2} - \cdots\right)\right] + K_s t \qquad (6.42)$$

where A_o, B_o, C_o, $\cdots$ are constants depending upon the soil hydraulic functions as well as θ_i and θ_S. The time derivative of (6.42) gives the infiltration rate

$$q_o = \frac{S}{A_o}\left[1 - \exp\left(-A_o t^{1/2} - B_o t - C_o t^{3/2} - \cdots\right)\right] \cdot \left[\frac{A_o}{2} t^{-1/2} + B_o + \frac{3}{2} C_o t^{1/2} + \cdots\right] + K_s \qquad (6.43)$$

Parlange (1971), realizing that Richard's equation originated from a combination of the Darcy-Buckingham equation and the equation of continuity, also obtained a solution. His original procedure consisting of iterative processes was gradually corrected by Císler (1974) and further modified (Parlange et al., 1982, and Parlange et al., 1985) to its present form. The procedure, based upon an integral moment balance (Raats, 1988), uses a double integration of the equation of continuity (6.2). The starting point is

$$\int_0^{-} \left(q - q_-\right) dz = \frac{\partial}{\partial t} \int_0^{-} \left(\theta - \theta_-\right) dz \qquad (6.44)$$

When the diffusivity form of the Darcy-Buckingham equation was combined with (6.44), Haverkamp et al. (1990) using two approximation steps obtained two well behaved equations. Owing to this contribution of Parlange and Haverkamp, we call them the P-H equations. In their dimensionless form they are

$$I^* = \frac{\gamma}{q_o^* - 1} + (1-\gamma)\ln\left[1 + \frac{1}{q_o^* - 1}\right] \tag{6.45}$$

and

$$t^* = (1-2\gamma)\ln\left[1 + \frac{1}{q_o^* - 1}\right] + \frac{\gamma}{q_o^* - 1} - \frac{1-\gamma}{q_o^*} \tag{6.46}$$

where

$$q^* = \frac{dI^*}{dt^*},$$

$$I^* = \left[1 - K_i t\right]\frac{2(K_S - K_i)}{S^2 + 2K_i h_o(\theta_S - \theta_i)},$$

$$t^* = \frac{2(K_S - K_i)^2 t}{S^2 + 2K_i h_o(\theta_S - \theta_i)}$$

and

$$\gamma = \frac{2K_S(h_o - h_W)(\theta_S - \theta_i)}{S^2 + 2K_i h_o(\theta_S - \theta_i)}.$$

The value of h_W is the water entry value on the wetting branch of the SWRC. After I^* and t^* are computed for chosen values of q^*, all three terms are transformed back to the dimensional forms I, q and t.

The integral method can also involve a mass balance formulation where (Raats, 1988)

$$\int_0^t \left[q_o(t) - q_{-\infty}\right] dt = \int_{\theta_i}^{\theta_s} z\,(\theta, t\,)\, d\theta \tag{6.47}$$

which is also obtained by integrating the equation of continuity. Philip (1973) and Philip and Knight (1974) managed to reduce the number of independent variables of the infiltration problem by using a guessed shape for the ratio of flux densities q/q_o. The main idea of this "flux-concentration relation" method is explained in more detail in section 6.2.3.2.

The parameterized flux density F related to the parameterized water content θ_R for *horizontal infiltration* is

$$F(\theta_R, t\,) = \frac{q}{q_o} \tag{6.48}$$

or with (6.32)

$$F(\theta_R) = \frac{\int_{\theta_i}^{\theta} \eta(\theta)\, d\theta}{\int_{\theta_i}^{\theta_s} \eta(\theta)\, d\theta} \tag{6.49}$$

where

$$\theta_R = \frac{\theta - \theta_i}{\theta_S - \theta_i}.$$

Relation (6.49) is the ratio of the partial and total sorptivities calculated from (6.32) and illustrated in Fig. 6.13. $F(\theta_R, t)$ is the guessed shape which is inserted into the diffusivity form of the Darcy-Buckingham equation to obtain

$$F(\theta_R, t\,) = -\frac{D(\theta)}{q_o}\frac{\partial \theta}{\partial x}. \tag{6.50}$$

With

$$q_o = \frac{1}{2} S t^{-1/2}$$

the sorptivity is (Philip and Knight, 1974)

$$S = \left[2 \int_{\theta_i}^{\theta_s} \frac{(\theta - \theta_i) D(\theta)}{F(\theta_R)} d\theta \right]^{1/2} \quad (6.51)$$

If $F(\theta_R)$ is known, the above solution is available. Inasmuch as the time dependence of $F(\theta_R)$ is neglected, the solution is approximate. Philip (1973) has demonstrated that $F(\theta_R)$ can only exist within a relatively narrow domain. In Fig. 6.14 it can be seen that the domain is limited on one side by the curve which represents a linear soil having a constant D and from the other side by the straight line ($F = \theta_R$) which is descriptive of a soil having a $D(\theta)$ equal to a Dirac δ-function. For $\theta_R = 0$, $F = 0$, and for $\theta_R = 1$, $F = 1$. These two soils should represent the extremes of existence of $D(\theta)$ for real soils. Although the difference between the $F(\theta_R)$ relationships for these two soils appears slight in Fig. 6.14, their soil water content distributions for horizontal infiltration are strikingly different, see Fig. 6.16.

For vertical infiltration (6.48) is modified to

$$F(\theta_R, t) = \frac{q - K_i}{q_o - K_i} \quad (6.52)$$

and the $F(\theta_R)$ relationships for the two extreme soils are given in Fig. 6.15.

The solutions for the two extreme soils have the typical features of a theoretical treatment with no direct applicability to reality. Linear soil, characterized by a constant D and a K proportional to θ_R leads to h being proportional to $\ln\theta_R$ - a relationship for a SWRC which is not realistic for soils or other porous media. It would appear that for δ-function soils, infiltration should be easily approximated owing to the steep rise of D with θ_R and that $F(\theta_R) = \theta_R$ looks like a good approximation for the ratio of flux densities. However, when the sorptivities computed for δ-function soils were compared

to those obtained analytically for soils having a very steep $D(\theta)$, relative errors exceeded 20% (Kutílek and Valentová, 1986). Therefore, for most soils the iterative procedures proposed by Philip and Knight (1974) should be adopted.

In order to obtain solutions for models characteristic of real soils, proper functional relationships $D(\theta)$, $K(\theta)$ and $h(\theta)$ are required. To obtain them Richard's equation is linearized with transformations, e. g. those of Storm or Hopf and Cole. A review of such solutions identifying the authors of each transformation is provided by Raats (1990).

6.2.2.3 Approximate Solutions

The solution of the infiltration process, approximated physically or mathematically, is usually not kept wholly within either category but relies more heavily upon one or the other. A physical approximation is dominant in the procedure of Green and Ampt (1911) while mathematical approximations prevail in remaining, more recent procedures.

Green and Ampt (1911) simplified a real soil water profile of infiltration to a step-like profile, see Fig. 6.17. In this model, water penetrates into the soil like a piston which proceeds with time to greater depths. Below the abrupt, horizontal wetting front, the soil remains dry at its initial value of $\theta = \theta_i$. In the saturated upper part of the soil, flow is now simply described by Darcy's equation. If at time t the position of the wetting front is $z = L_f$ (the thickness of the soil saturated with water is also L_f), the infiltration rate is

$$q_o(t) = -K_s \left\{ \frac{h_f - [h_o - L_f(t)]}{L_f(t) - 0} \right\} = K_s \left\{ \frac{h_o + L_f(t) - h_f}{L_f(t)} \right\} \quad (6.53)$$

where h_o is the pressure head at the soil surface (i. e., the depth of water on the surface). Note that L_f is time dependent. The term h_f is the soil water pressure head at the wetting front owing to the unsaturated condition of the soil below z with $h_f < 0$. If there were no soil below $z = L_f$ and water was falling out of the saturated soil column ($h = 0$ at $z = L_f$), the water flux throughout the column of thickness L_f would be

$$q_o = q = K_s \frac{h_o + L_f(t)}{L_f},$$

see Fig. 6.17. Because there is dry soil below $z = L_f$, its unsaturated condition causes the flux to increase. Green and Ampt added the term h_f to the driving force to account for the extra force acting at the wetting front. Neuman (1976) has shown that

$$h_f = \frac{1}{K_s}\int_0^{h_i} K(h)\,dh \tag{6.54}$$

and

$$h_f = \frac{1}{K_s}\int_{\theta_i}^{\theta_s} D(\theta)\,d\theta \tag{6.55}$$

Or, using the Parlange (1975) solution

$$h_f = \frac{1}{2}\int_0^{h_i}\left(\frac{\theta_s - \theta(h) - 2\theta_i}{\theta_s - \theta_i}\right)\left[\frac{K(h)}{K_s}\right]dh \tag{6.56}$$

Obviously, without knowing the original publication of Green and Ampt, Budagovskij (1955) based his monographic study upon the same principle.

Theoretically, the procedure is based upon the expected shape and similarity of the $\theta(z, t)$ profiles. Philip (1957, 1973) showed that the following Green and Ampt approximation is an exact solution only if $D(\theta)$ is expressed as a Dirac δ-function. Considering (6.53), we know $q_o = dI/dt$ and $I = L_f\Delta\theta$ where $\Delta\theta = \theta_S - \theta_i$, and hence,

$$q_o = \frac{dL_f}{dt}\,\Delta\theta \tag{6.57}$$

When the force of gravity is neglected, i. e. for horizontal infiltration, substituting (6.57) into (6.53), we have

$$\frac{dL_f}{dt}\,\Delta\theta = K_s\left(\frac{h_o - h_f}{L_f(t)}\right), \tag{6.58}$$

and after separating variables

$$\int_0^{L_f} L_f\,dL_f = \int_0^t K_s\left(\frac{h_0 - h_f}{\Delta\theta}\right)dt \tag{6.59}$$

After integrating,

$$L_f = \left[2K_s\left(\frac{h_0 - h_f}{\Delta\theta}\right)\right]^{1/2} t^{1/2} \tag{6.60}$$

or with $L_f = I/\Delta\theta$,

$$I = \left[2K_s(h_o - h_f)\Delta\theta\right]^{1/2} t^{1/2} \tag{6.61}$$

Comparing (6.61) with (6.33), we obtain the sorptivity S

$$S = \left[2K_s(h_o - h_f)\Delta\theta\right]^{1/2} \tag{6.62}$$

Equation (6.61) can also be used to estimate absorption during a brief initial period of vertical infiltration. Equation (6.62) defines approximately how S depends upon θ_i.

When gravity is not neglected, (6.53) becomes

$$\Delta\theta\,\frac{dL_f}{dt} = K_s\left\{\frac{L_f(t) + (h_o - h_f)}{L_f(t)}\right\}. \tag{6.63}$$

After separating variables and integrating between the limits $(0, t)$ and $(0, L_f)$, we obtain

$$t = \frac{\Delta\theta}{K_s}\left\{L_f - \left(h_o - h_f\right)\ln\left[1 + \frac{L_f}{\left(h_o - h_f\right)}\right]\right\}. \qquad (6.64)$$

Notice that this solution does not allow $I(t)$ to be described explicitly. Such an implicit transcendental function is typical for all solutions embracing the Green and Ampt approach even when it is not apparent in some more sophisticated developments. When (6.64) is transformed with dimensionless terms

$$t^* = \frac{K_s t}{\Delta\theta\left(h_o - h_f\right)} \qquad (6.65a)$$

and

$$I^* = \frac{I}{\Delta\theta\left(h_o - h_f\right)} \qquad (6.65b)$$

we have

$$t^* = I^* - \ln\left(1 + I^*\right) \qquad (6.66)$$

which can be evaluated graphically (see Fig. 6.25) or by computing t for a series of values of L_f with $I = L_f\Delta\theta$.

Because the procedure is simple, the Green and Ampt approximation has been widely used in research as well as in the solution of many practical engineering problems. It has also been applied to the description of infiltration into layered profiles and those having a crust surface. However, we have to keep in mind that real soils do not manifest a δ-function $D(\theta)$, and hence, the method offers results of disappointingly poor accuracy. For example, the error involved in predicting $I(t)$ or $q_o(t)$ can approach 30 %. Its use should be limited to those wanting only a convenient, rough estimate of infiltration.

Within the second category of approaches, Philip's (1957b) algebraic infiltration equation is the most common. This approximate equation is merely

the first two terms of the series solution (6.38) with the cumulative infiltration $I(t)$ being

$$I = St^{1/2} + At \qquad (6.67)$$

and the infiltration rate q_o ($= dI/dt$) being

$$q_o = \frac{1}{2}St^{-1/2} + A. \qquad (6.68)$$

These equations like their parent time series solution (6.38), are applicable to relatively short times. The magnitude of A is $(A_2 + K_i + \varepsilon)$ where ε is the truncation error for having used only the first two terms of (6.38). It was expected that A be related to K_S by a simple, sufficiently accurate relation $A = mK_S$. Although the most frequently used value of m is 2/3, its value ranges between 0.2 and 0.67 (Philip, 1987). However, detailed studies show that m depends upon both θ_i and time and sometimes exceeds a theoretical upper limit of 2/3. The error of estimate of K_S derived from A could theoretically reach about 30% in a relatively dry homogeneous soil (Kutflek et al., 1988). Therefore, (6.67) cannot be reliably used for estimating the value of K_S from infiltration tests.

Sorptivity S in (6.67) and (6.68) is an estimate of the theoretical value of sorptivity for a soil having initial water content θ_i. The truncation error influences the estimated value of the sorptivity to a lesser degree than that of A. Thus, S evaluated from the early stage of infiltration is considered a reliable value (Kutflek et al., 1988).

In order to reduce the truncation error, Kutflek and Krejča (1987) proposed to use three terms of the time series solution (6.38)

$$I = C_1 t^{1/2} + C_2 t + C_3 t^{3/2} \qquad (6.69)$$

where C_1 is the estimate of sorptivity S, C_2 the estimate of $(A_2 + K_i)$ and C_3 the value of $(A_3 + \varepsilon_1)$ where ε_1 is the truncation error for having used three terms of

(6.38). If we approximate the limiting time for which the truncated series (6.69) converges as the value of t when $dq_o/dt \rightarrow 0$, we have

$$t_{lim} = \frac{C_1}{3C_3}. \tag{6.70}$$

And, if we make an additional approximation that $q_o(t_{lim}) \approx K_S$, we obtain the estimate

$$K_S \approx (3C_1C_3)^{1/2} + C_2 \tag{6.71}$$

Simplifying (6.42) in a manner similar to (6.67), Swartzendruber (1987) suggested using

$$I = \frac{S}{A_o}\left[1 - \exp\left(-A_o t^{1/2}\right)\right] + K_S t. \tag{6.72}$$

Substituting $4K_S/3S$ for A_o into the above equation, we obtain the two-parameter infiltration equation proposed by Stroosnijder (1976). On the other hand, if we consider only the first four terms of a series expressing the exponential term $\exp(-A_o t^{1/2})$, we obtain an equation identical to (6.69).

Equations (6.69) and (6.72) have similar disadvantages. Parameters C_2, C_3 and A_o are not simply calculated or predicted from known hydraulic functions K_S, $K(h)$ and $\theta(h)$. When those equations are used for estimating S and K_S from measured values of $I(t)$, the estimates are reliable only for a strictly homogeneous soil column with an initial condition $d\theta_i/dz = 0$. When the equations are applied to field data, significant, intolerable errors are sometimes apparent. For example, when K_S is being evaluated, physically unreal values of $K_S < 0$ are sometimes obtained (Kutílek and Krejča, 1987, and personal communication from Krejča, 1989).

Brutsaert (1977) also began with the horizontal solution of Philip (1957) and subsequently sought a correction for the gravitational force. He obtained

$$I = K_S t + \frac{S^2}{BK_S}\left\{1 - \frac{1}{\left[1 + \left(BK_S t^{1/2}\right)/S\right]^2}\right\} \tag{6.73}$$

and

$$q_o = K_S + \frac{1}{2} S t^{1/2}\left\{\frac{1}{\left[1 + \left(BK_S t^{1/2}\right)/S\right]^2}\right\}. \tag{6.74}$$

He considered values of $B = 1/3$, $2/3$ or 1 each descriptive of physical reality, but for most practical purposes, recommended $B = 1$. Values of $I(t)$ computed with (6.73) are nearly identical to those from (6.38) when the hydraulic functions of the soil are known. And, inversely, estimates of S and K_S from the experimental data using (6.73) appear more reliable than those using other approximate equations based on comparative theoretical errors.

From this and the previous section, we conclude that both $I(t)$ and $q_o(t)$ can be quickly and reliably computed for trivial initial and boundary conditions with (6.45) and (6.46) or (6.73) and (6.74), respectively. The value of S is advantageously obtained using the approximate expression of Parlange (1975)

$$S = \left[\left(\theta_S - \theta_i\right)\int_{\theta_i}^{\theta_S} D(\theta)\,d\theta + \int_{\theta_i}^{\theta_S}\left(\theta - \theta_i\right) D(\theta)\,d\theta\right]^{1/2} \tag{6.75}$$

or the iterative procedure described by Philip and Knight (1974) or by White (1989) for the solution of (6.51).

From the authors' experience, increasing the number of parameters brings a theoretical improvement especially when soil hydraulic characteristics are evaluated from infiltration tests. For example, if we deal with approximate equations based upon the infinite series solution, the truncation error is reduced with an increased number of terms. However, equations with three or more parameters are more vulnerable to the field soil not being homogeneous and the boundary conditions deviating from the trivial ones assumed in the theoretical development. This vulnerability is realized when a number of

physically non-realistic parameters are obtained (e. g. a negative value of K_S in the inverse solution).

6.2.2.4 Empirical Equations

Historically, empirical equations have been used to describe a decreasing infiltration rate q_o as a function of time t. The shape of a smooth curve drawn through measured values of $q_o(t)$ was simply compared with that of an analytic function. Inasmuch as both equations and experiments were empirical, it is useless to try to physically interpret the coefficients of the equations. The coefficients have the character of fitting parameters only with no scientific merit (Haverkamp et al., 1988, and Kutílek et al., 1988). On the other hand, because of their popularity in the literature and their usage persists, we briefly present them here.

Kostiakov's (1932) equation of $q_o(t)$ is the hyperbola

$$q_o = c_1 t^{-\alpha} \tag{6.76}$$

with

$$I = \frac{c_1}{1-\alpha} t^{(1-\alpha)} \tag{6.77}$$

where c_1 and α are empirical coefficients The value of c_1 should equal q_{o1}, the infiltration rate at one unit of time (usually 1 min), and $0 < \alpha < 1$. The equation does not describe infiltration at large times inasmuch as $q_o \to 0$ when $t \to \infty$. Mezencev (1948) overcame this inconvenience by shifting the q_o-axis

$$q_o = c_2 + c_3 t^{-\beta} \tag{6.78}$$

with

$$I = c_2 t + \frac{1}{1-\beta} c_3 t^{(1-\beta)} \tag{6.79}$$

where c_2, c_3 and β are empirical coefficients. With the shift, as $t \to \infty$, $c_2 \to q_{oc}$, the constant infiltration rate when quasi-steady infiltration is reached, and hence, $q_{oc} = K_S$. The infiltration rate after the first time unit $q_{o1} = (c_2 + c_3)$.

Horton's equation (1940) represents an exponential decay of $q_o(t)$

$$q_o = c_4 + c_5 \exp(-\gamma t) \tag{6.80}$$

with

$$I = c_4 t + \frac{c_5}{\gamma}\left[1 - \exp(-\gamma t)\right] \tag{6.81}$$

where c_4, c_5 and γ are empirical coefficients. In contradiction to the theory of infiltration for a DBC, q_o has a finite value at $t = 0$. As $t \to \infty$, $c_4 \to q_{oc}$ which yields a value of $c_4 = K_S$. With this approximation for K_S, the value of $c_5 = [q_o(0) - K_S]$ where $q_o(0)$ is q_o at $t = 0$. Inasmuch as Horton derived his equation for infiltration of a high intensity rainfall, the physical objection against a finite value of $q_o(0)$ is largely eliminated as we shall see in the next section.

Holtan's equation (1961) for a decay of q_o with I is

$$q_o = c_6 (W - I)^{\varepsilon} + c_7 \tag{6.82}$$

where c_6, c_7 and ε are empirical coefficients, $c_7 = q_{oc}$, W is soil water storage above an impeding layer and ε, not an integer, is most frequently greater than unity. Equation (6.82), incorporated into the USDA Hydrograph Laboratory model USDAHL, has empirical coefficients related to the soil mapping units in USA (Holtan and Lopez, 1971).

Sept 1993

6.2.3 Unsteady Infiltration, Neuman's Boundary Condition (NBC)

When we describe rainfall infiltration, we consider that the REV is defined at the Darcian scale. Therefore, we do not describe individual raindrop events, but consider the rain as a continuous flux with the intensity of the rain q_r being the flux density passing either totally or at least partially through the surface of the soil. The boundary condition at $z = 0$ and $t \geq 0$ is formulated by the Darcy-Buckingham equation (5.31)

$$q_o = -K \frac{\partial H}{\partial z} \tag{6.83a}$$

or in diffusivity form (5.68a)

$$q_o = K(\theta) - D(\theta) \frac{\partial \theta}{\partial z} \tag{6.83b}$$

Condition (6.83), called Neuman's boundary condition, describes not only rainfall infiltration, but infiltration caused by sprinkler irrigation or by a special flux controlled technique, e. g. by a peristaltic pump providing a constant flux through a membrane placed upon the soil surface. For drip irrigation, we have a 2-dimensional problem with boundary conditions appropriately modified. Field measurements of infiltration with boundary conditions (6.83) are usually performed with rain simulators, see a review of Amerman (1983). Nozzles or hypodermic needles are used to produce drops similar to raindrops at a certain height above the soil surface. Regardless of how boundary condition (6.83) is achieved, the initial condition is kept the same as that for the DBC.

6.2.3.1 Description of the Process

We denote this description into the three categories (i) constant rain intensity $q_r > K_S$, (ii) constant rain intensity $q_r < K_S$ and (iii) rain intensity $q_r(t)$. In all three categories soil water profiles $\theta(z)$ at intermediate times do not resemble $\theta(z)$ during early stages of infiltration. The distinguishing feature is that the soil water content $\theta_o(t)$ increases at the surface with time.

(6.18)

Constant rain intensity $q_r > K_S$. The value of the soil water content of the surface θ_o increases steeply with time until it reaches θ_S, see Fig. 6.18. The greater is q_r, the steeper is $\theta_o(t)$. If rain continues, water ponds on the surface and the start of ponding is called ponding time t_p. If surface runoff is prevented, the depth of water on the surface $h_o(t)$ increases with time and $h_o > 0$ for $t > t_p$. With the increase of h_o being time dependent, $dh_o/dt < q_r$. The shape of the soil water profile at $t < t_p$ depends upon both q_r and the hydraulic functions of the soil, see Fig. 6.22. For $t = t_p$ the thickness of the saturated zone L_f extending below the soil surface is (Rubin and Steinhardt, 1964)

$$L_f = a \left(\frac{h_A K_S}{q_r - K_S} \right) \tag{6.84}$$

where a is an empirical parameter. For $t \geq t_p$ the soil water profile $\theta(z, t)$ resembles the profile with a DBC, i. e. with water ponded on the soil surface. Hence, we specify the boundary conditions as follows

$$q_r = K(\theta) - D(\theta) \frac{\partial \theta}{\partial z} \qquad z = 0 \qquad 0 < t < t_p \tag{6.85}$$

$$\theta = \theta_S \qquad z = 0 \qquad t \geq t_p \tag{6.86}$$

or, more exactly

$$h = 0 \qquad z = 0 \qquad t = t_p \tag{6.87}$$

and either

$$h = 0 \qquad z = 0 \qquad t > t_p \tag{6.88}$$

or

$$h = h_o(t) \qquad z = 0 \qquad t > t_p \tag{6.89}$$

Ponding time t_p separates the infiltration event into two different periods. The first is governed by the NBC (6.85) while the second is governed by the DBC

(6.86) or (6.87) to (6.89).

6.2.3.2 Approximate Solutions

For an approximate intuitive derivation of t_p we compare infiltration for a DBC with that for a NBC. The parameters will be indexed by D for DBC and by N for NBC. Rubin (1966) has shown that the ponding time t_p decreases with q_r and that $t_p > t_x$ where t_x is the intersection of q_r and q_D, see Fig. 6.19. In order to satisfy boundary conditions (6.85) and (6.86) as the NBC transforms to DBC, we assume the soil water profiles $\theta(z, t_p)_N$ and $\theta(z, t_x)_D$ are identical. Hence, $I_N(t_p) = I_D(t_x)$. The cumulative infiltration is also

6.19

$$\int_0^{t_p} q_r(t)\,dt = \int_0^{t_x} q_D(t)\,dt \tag{6.90}$$

With q being continuous, we recognize that

$$q_r(t_p) = q_D(t_x) \tag{6.91}$$

and for a constant value of q_r we obtain

$$t_p = \frac{1}{q_r}\int_0^{t_x} q_D(t)\,dt \tag{6.92}$$

where t_x is the time at which q_r and q_D intersect. Graphical interpretation of (6.90) and (6.91) is given in Fig. 6.19. With $q_D(t)$ expressed by Philip's approximate algebraic equation (6.68), Kutílek (1980) obtained

$$t_p = \left(\frac{S}{A}\right)^2 \frac{2Q_r^* - 1}{4Q_r^*\left(Q_r^* - 1\right)^2} \tag{6.93}$$

where $Q_r^* = q_r / A$. Similarly, $q_D(t)$ from other approximate solutions can be used to calculate t_p.

At $t \le t_p$ the infiltration rate $q_o = q_r$. At $t > t_p$ the infiltration rate can be approximated by shifting $q_D(t)$ by $(t_p - t_x)$. With (6.92) and with

$$t_x = \left(\frac{S}{A}\right)^2 \frac{1}{4\left(Q_r^* - 1\right)^2} \tag{6.94}$$

we obtain the infiltration rate $q_o(t)$ for $t > t_p$

$$q_o = \frac{1}{2} S \left[t - \frac{S^2}{4A^2 Q_r^*\left(Q_r^* - 1\right)}\right]^{-1/2} + A. \tag{6.95}$$

All of the above approximations as well as many others in the literature have two disadvantages. First, the equality $I_N(t_p) = I_D(t_x)$ is just an assumption teoretically derived by Mls (1980) and the same is for post-ponding infiltration rates when they are computed as simple translations of the rate q_D. Second, the simple explicit formulation of $q_D(t)$ is, in reality, only an approximation. Therefore, the purpose of our above discussions was to illustrate as simply as possible the nature of infiltration under two different boundary conditions. The equations can be used for rough engineering estimations provided that the soil surface quality is not altered during the process, see section 6.2.4.1.

Constant rain intensity $q_r < K_S$. Here, the value of the soil water content on the surface $\theta_o(t)$ increases similarly to the first case but its limiting value is $\theta_f < \theta_S$. Inasmuch as $dH/dz \to -1$ at the soil surface as $t \to \infty$, we obtain a quasi-steady infiltration rate $q_o = q_r = K(\theta_f)$. And, the value of $\theta_o(t)$ approaches θ_f asymptotically in time, see Fig. 6.20. The shapes of the soil water profile vary with both time and infiltration rate. In Fig. 6.22 we see the importance of the hydraulic characteristics of the soil for a constant infiltration rate at different times. This example from Broadbridge and White (1988) is for two different forms of the SWRC which are derived from the solution having an empirical coefficient C. The influence of the value of C upon the shape of the SWRC is shown in Fig. 6.22. The details of the solution are described by the authors.

6.20

Non-constant rain intensity $q_r(t)$ When $q_r(t)$ is strongly time dependent as it is in a great majority of heavy rainfalls, we obtain an estimate of t_p using the procedure described for a constant value of $q_r > K_S$. Equations (6.90) and (6.91) can be solved iteratively. Or, if $q_r(t)$ is capable of being expressed as a probability

distribution function, we can solve them analytically. Regardless of the procedure, we recall that the solution remains only an approximation owing to the use of $q_D(t)$. Figure 6.21 shows the example of the graphical solution of (6.90) and (6.91) for ponding time t_p. By simply shifting q_D by $(t_p - t_x)$ we obtain estimates of the infiltration rate for $t > t_p$ and the hydrologically effective rainfall. The same priciple was applied for a histogram of rainfall intensity. Details regarding the construction or computation are described by Peschke and Kutflek (1982).

(6.21)

White et al. (1989) proposed the approximate analytic solution

$$t_p = \frac{1}{\bar{q}_r} M \frac{S^2}{K_S} \ln\left[\frac{q_r(t_p)}{q_r(t_p) - K_S}\right] \tag{6.96}$$

where $\bar{q}_r$ is the mean q_r during the time interval $(0, t_p)$ and $0.5 \le M \le 0.66$. More than a decade earlier Parlange and Smith (1976) had derived a very similar expression. Both expressions have features like those of the Green and Ampt solution. In order to avoid redistribution, these expressions require $q_r(t)$ not to decrease, see section 6.3.

6.2.3.3 Analytical Solutions

If we neglect early approximate solutions based upon the Green and Ampt approach (e. g. Mein and Larson, 1973), four scientists eventually achieved an analytical solution for t_p. Parlange (1972) provided the initial effort which was subsequently modified by Philip (1973) and by Philip and Knight (1974). Philip and Knight utilized the concept of "flux concentration relation" [for convenience, (6.52) is repeated here]

$$F(\theta_R, t) = \frac{q - K_i}{q_o - K_i}$$

and neglected its time dependence which is even weaker than that for the DBC. When the above expression for $F(\theta_R, t)$ is inserted into the diffusivity form of the Darcy-Buckingham equation (5.68a)

$$q = -D(\theta)\frac{\partial\theta}{\partial z} + K(\theta) \tag{6.97}$$

we obtain with $q_o = q_r$

$$F(\theta_R)(q_r - K_i) - \left[K(\theta) - K_i\right] = -D(\theta)\frac{\partial\theta}{\partial z}. \tag{6.98}$$

Integrating from $z = 0$ yields

$$z = \int_{\theta_i}^{\theta_o(t)} \frac{D(\theta)\,d\theta}{F(\theta_R)(q_r - K_i) - \left[K(\theta) - K_i\right]} \tag{6.99}$$

where $\theta_o(t)$ remains unknown. Integrating the equation of continuity (5.65) with q_r constant between the limits $(0, t)$ and $(0, z)$ gives

$$-(q_r - K_i)t = \int_{\theta_o(t)}^{\theta_i} z\,d\theta \tag{6.100}$$

Combining (6.99) and (6.100) and integrating leads to

$$(q_r - K_i)\,t = \int_{\theta_i}^{\theta_o(t)} \frac{(\theta - \theta_i)\,D(\theta)\,d\theta}{F(\theta_R)(q_r - K_i) - \left[K(\theta) - K_i\right]} \tag{6.101}$$

From (6.101) the evolution of the water content of the soil surface $\theta_o(t)$ is ascertained. When we know θ_o for a particular time t, we compute the soil water profile $\theta(z)$ from (6.99). If $q_r > K_S$ we compute the ponding time t_p from (6.101)

$$t_p = \frac{1}{q_r - K_i}\int_{\theta_i}^{\theta_o(t)} \frac{(\theta - \theta_i)\,D(\theta)\,d\theta}{F(\theta_R)(q_r - K_i) - \left[K(\theta) - K_i\right]} \tag{6.102}$$

A detailed step-by-step development of the procedure shows that the authors treat component equations of the Richards equation and integrated the Darcy-Buckingham equation by using a guessed shape of the flux concentration relation $F(\theta_R)$.

Proper judgment for an appropriate value of $F(\theta_R)$ is critical. Philip's (1973) calculations of $F(\theta_R)$ for horizontal infiltration into linear and δ-function soils lead to approximations for early stages of infiltration limited to values of $q_r \approx K_S$. Another approximation for a constant flux infiltration was found assuming $F(\theta_R) = \theta_R^n$ with $0.8 \leq n \leq 1$ (Kutflek, 1980, Perroux et al., 1981, and Boulier et al., 1984). In general, errors associated with the uncertainty in $F(\theta_R)$ are less than those owing to our uncertainty in estimating $D(\theta)$. Considering the joint development of (6.102), the procedure should be called the Parlange-Cîsler-Philip-Knight (PCPK) method' see our introductory remarks and comments to (6.44) and (6.47).

Morel-Seytoux (1982) also provided an acceptable approximation for a constant intensity rainfall. For a variable rainfall his solution is restricted to soils having $K/K_S = \theta_R^n$ and to that initial part of a rainfall when its intensity is increasing with time. His method cannot be applied to the receding part of rainfall inasmuch as the procedure does not consider θ_0 decreasing as water redistributes within the profile. Generally, infiltration stemming from a variable rainfall can only be accommodated by numerical procedures.

The most versatile analytical solution of constant rate infiltration was published by Broadbridge and White (1988). They allowed the soil hydraulic functions to exist in broad limits between those of linear and δ-function soils. The hydraulic functions typical of real soils are expressed by a simple, free parameter C which is easily measured in the field. A detailed description of the procedure involving Kirchoff, Storm, Hopf and Cole and Laplace transformations is beyond the scope of this book. Their strictly analytical solution in parametric form given in Fig. 6.22 is most useful for testing numerical schemes. Moreover, the application of their solution to practical examples contributed to our knowledge of infiltration discussed in the previous section.

(6.22)

Numerical solutions have been reviewed by Vauclin et al. (1979) and van Genuchten (1981). Among improvements provided in the last decade are those of Mls (1982).

6.2.4 Field Infiltration

When field infiltration tests are performed and evaluated, we meet a complex set of effects not fully accounted for by exactly defined infiltration equations. These effects more or less influence the observed data and the applicability of infiltration theory to runoff hydrology, irrigation and other practical domains involving infiltration. Some of these effects will be discussed.

6.2.4.1 Soil Sealing and Crusting

During *ponded infiltration* tests (DBC), the abrupt contact of the soil surface with excess water causes weak aggregates to disintegrate and slake. The migrating smaller particles quickly form a seal on the soil surface within a short period of only a few minutes. The slaked clay particles are gel-like and exhibit a thixotropic behavior not yet fully studied in detail. We expect in the presence of mono-valent cations that this peptization of clays leads to the separation of individual sheets of clay minerals that subsequently reorient into horizontal, parallel configurations that tend to seal the soil surface causing an extremely small value of K_S. Bi-valent cations allow the clay sheets to remain coagulated and in a face-to-edge configuration. Hence, the value of K_S of the seal for bi-valent cations is larger than that for mono-valent cations, but nevertheless orders of magnitude less than that of the original soil. The value of K_S of the seal and its thickness are both time dependent. The formation and quality of this seal are major factors responsible for the difference in infiltration rates between structured and structure-less soils, see Fig. 6.23. Surface sealing is not a rare phenomenon - indeed, it occurs with virtually all arable soils during ponded infiltration.

(6.23)

During *rainfall infiltration*, the slaking of aggregates is enhanced by the kinetic energy of the raindrops. The impact of raindrops upon the soil surface can be compared to a micro-bombardment. The drop after hitting the soil forms a micro-crater with some of the segregated fine soil particles relocating to clog pores and the remainder washed deeper into the soil with the infiltrating water. Inasmuch as the ponding time differs from one point to another, suspended clay particles are transported to small puddles and unevenly deposited across the soil surface. During the subsequent dry period after the rain, the newly

formed seal consolidates and forms a crust. With repetitive rainfalls the process of sealing and crusting eventually forms a crust-topped soil. For such a soil crust, McIntyre (1958a and 1958b) defined two layers - a compacted thin layer called a skin and a less dense "washing-in layer". For an originally undisturbed soil having a value of K_S = 36 mm/h, he reported a 0.1 mm thick skin having a K_S = 0.018 mm/h and a 1.5 to 2.5 mm "washing-in layer" having a value of K_S = 0.115 mm/h.

Mualem et al. (1990) defined two types of crusts. *Depositional crusts* are formed by fine particles settling from a suspension reaching a depositional site. The scale of this type of crust is related to the scale of observation. *Structural crusts* are caused by the destruction of soil aggregates exposed to the direct impact of raindrops as we discussed in the paragraph above.

Soil surface seals have relatively large values of bulk density ρ_T. The rate of increase of ρ_T depends upon the kinetic energy of the rain, nature of the soil and its aggregates and initial values of bulk density ρ_{Ti}. The smaller is ρ_{Ti}, the larger is the rate of change of $d\rho_T/dt$. Similar relations hold for K_S and other hydraulic functions of the seal.

Seal formation is more dependent upon rainfall energy than upon cumulative rainfall. Rainfall energy is closely correlated with rain intensity. The kinetic energy of rain which induces seals and crusts ranges from about 0.1 $J \cdot s^{-1} m^{-2}$ for a rain intensity q_r of about 0.3 $mm \cdot min^{-1}$ to 1.2 $J \cdot s^{-1} m^{-2}$ for q_r = 2.5 $mm \cdot min^{-1}$.

Once a seal is developed by a rain event, the physical properties of the seal are usually sustained. Repeated high intensity rainfall or sprinkler irrigation forms deleterious, undesirable crusts in the majority of agricultural soils. For example, below a 5 mm thick surface crust, Passerat de Silans et al. (1989) measured values of ρ_T = 1.32 $g \cdot cm^{-3}$ and K_S = 1.3 x 10^{-4} $m \cdot s^{-1}$. Within the crust ρ_T = 1.45 $g \cdot cm^{-3}$ and K_S = 2.8 x 10^{-6} $m \cdot s^{-1}$. Similar examples are reported in the literature, e. g. Callebaut et al. (1985). With the nature and extent of soil crusts being highly variable, their behavior falls between the one extreme of manifesting an earlier developed, constant hydraulic resistance and the other extreme of a gradually increasing hydraulic resistance as a seal develops during rainfall on an

Scientific colloquium

Porous or fractured unsaturated media: transports and behaviour

October 5 - 9 / 1992

Monte Verità, Centro Stefano Franscini - ETH - Zürich
Ascona, Switzerland

Organized by :

SWISS FEDERAL INSTITUTE OF TECHNOLOGY OF LAUSANNE (EPFL)

- **Land and Water Use Institute** (IATE)
- **Soil, Rock and Foundations Institute** (ISRF)

UNIVERSITY OF NEUCHATEL

- **Center of Hydrogeology** (CHYN)

Models of Soil Porous Systems for Unsaturated Flow

M. Kutílek, R. Rösslerová and H. Othmer

Abstract. The real soil fabric is characterized by the existence of peds up to the tertiary formation and by cutans covering the peds. Thus two or three porous systems are formed and the total soil porous system can not be modeled as homogeneous. The interpedal and intrapedal porous systems are hierarchically arranged. This type of arrangement is demonstrated by the macroscopic measurements on the Darcian scale (soil water retention curves and the unsaturated hydraulic conductivity functions). The microscopic percolation hierarchical models are applied for a more detailed discussion on the characteristics of the soil water retention curves of such systems.

1. Introduction

The soil porous system has been traditionally deduced from the soil water retention curve (SWRC) with the following assumptions : (i) SWRC is adequately formulated by an equation. (ii) The model of the soil porous system consists of parallel capillary tubes or, alternatively, of interconnected capillary tubes of basically parallel arrangement with a free access to the sources or sinks of the liquid for each capillary. (iii) The capillary model is micromorphologically homogeneous. All three assumptions are then incorporated in the routine procedures of the estimation of the unsaturated conductivity K and of the transport processes in general.

Soil micromorphology brings the contradictious evidence against the assumption (iii), i.e. against the homogeneity of the soil porous system. The real soil fabric is characterized by the existence of peds (aggregates) up to the tertiary formation and by cutans covering the peds (Fig. 1). Thus two or three porous systems are formed and the total soil porous system cannot be modeled as homogeneous. The models, assumption (ii), should therefore reflect the reality described by the soil micromorphology : the soil porous system is characterized by the hierarchical arrangement of the porous systems in peds (intrapedal pores) and the porous systems between the peds (interpedal pores). We suppose then that the pore size distribution is either bi– or n–modal. The equation of SWRC should be therefore used in a modified form in order to be consistent with the soil reality, see assumption (i). The shape of the interpedal pores should be related to the morphological features of the soil structure, too. However this is the task for the next research.

In this study we deal with the capillary porous systems in all instances. For pores where the capillarity exists we reserve the term micropores. The pores without detectable meniscus forces are denoted as macropores. The water flow in the microporous systems is described by the Richards' equation while the flow in the macroporous systems is described by the different type of equations, eg. by the kinematic wave equation (Germann and Beven, 1985). We decline here therefore from the earlier classification of pores as given in the review paper of Bouma (1991). The motive of doing so is in the use of two different types of equations applied.

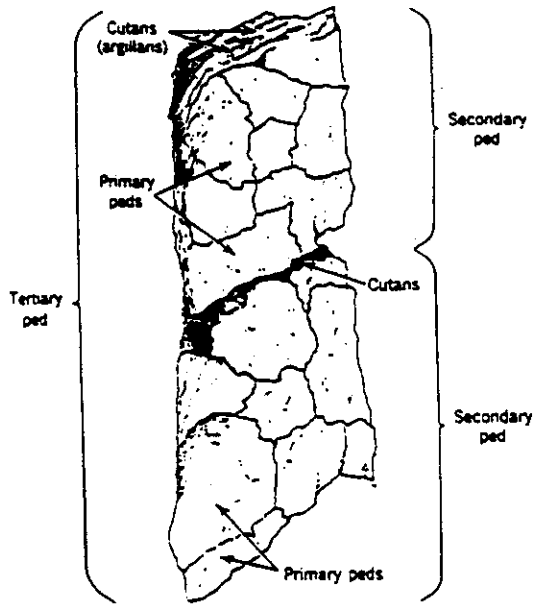

Fig. 1 The soil fabric : the primary peds formed by the soil solid constituents are arranged into the secondary and tertiary peds. The peds are covered by soil cutans (Brewer, 1964).

The interpedal pores are frequently included into the category of by-pass, or preferential pores due to their accelerated conductance of water and solutes, when they are compared to the transport in the intrapedal pores. The term dual porous system is frequently used, too. However, the criterion on the rate of the transport for the definition of the boundary between micropores and macropores is rather subjective and less applicable for the predictive models. In our terminology, the by-pass flow (preferential flow) can exist in microporous systems when the bi-modal porosity is detected.

2. Macroscopic studies

Here, we deal with the SWRC, $h(\theta)$ and with the unsaturated conductivity $K(\theta)$ or $K(h)$, where h is the matric (or soil water) potential expressed as pressure head (cm), θ is the volumetric soil water content (cm^3/cm^3). This part of our study is aimed at the macroscopic confirmation of the bi– or n–modal porosity and its influence upon the K(h) function. The study was a part of the investigation by a Special Collaborative Program, SCP 179 at the Technical University in Braunschweig.

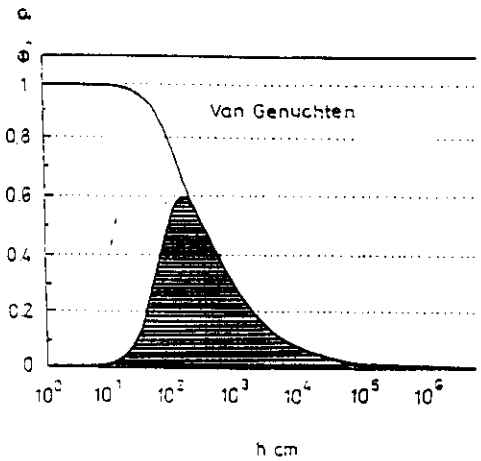

First, we shall assume in this chapter in accordance with the routine procedures that the derivative curve of the SWRC represents the pore size disribution with the equivalent pore radius $r = a/h$ with a, the constant. The derivative curve is identical with the PDF of r. The SWRC of soils of the mono-modal porosity is the curve with one peak representing the maximum frequency of the equivalent radius $r(p_{max})$, with p, the probability (Fig. 2).

Fig. 2 Soil water rentention curve and the pore size distribution of the mono-modal porous system.

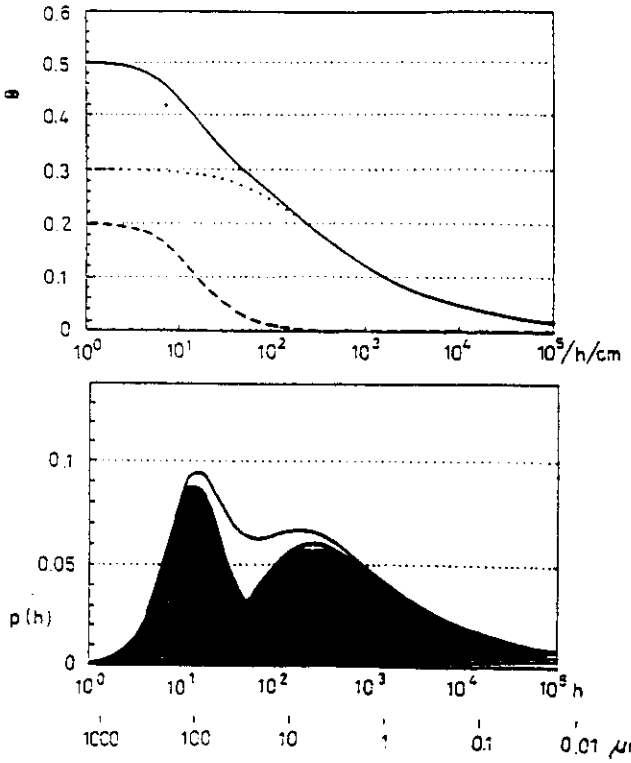

Fig. 3 Soil water retention curve and the pore size distribution of the bi-modal porous system.

The soils of the bi– or n–modal porosity have the derivative of the SWRC with two or n peaks (Fig. 3). It is assumed tacitly that all pores have the same free access to the draining pool of water and that the replacing air has the same opportunity to penetrate in all pores which are to be drained at the given pressure. Analogically for the wetting process, it is assumed that there is free access of water into all pores. The weak points of these assumptions will be discussed in the next chapter.

We have carefully analyzed the SWRC of our measured data on 250 cm^3 samples taken at the research base at Neuenkirchen close to Braunschweig.

First, we assumed the monomodal porous system. The experimental soil water retention – drainage data were fitted to the van Genuchten's equation (1980) – and we obtained smooth sigmoidal curves, each with one inflection point only. One example of all is in Fig. 4a.

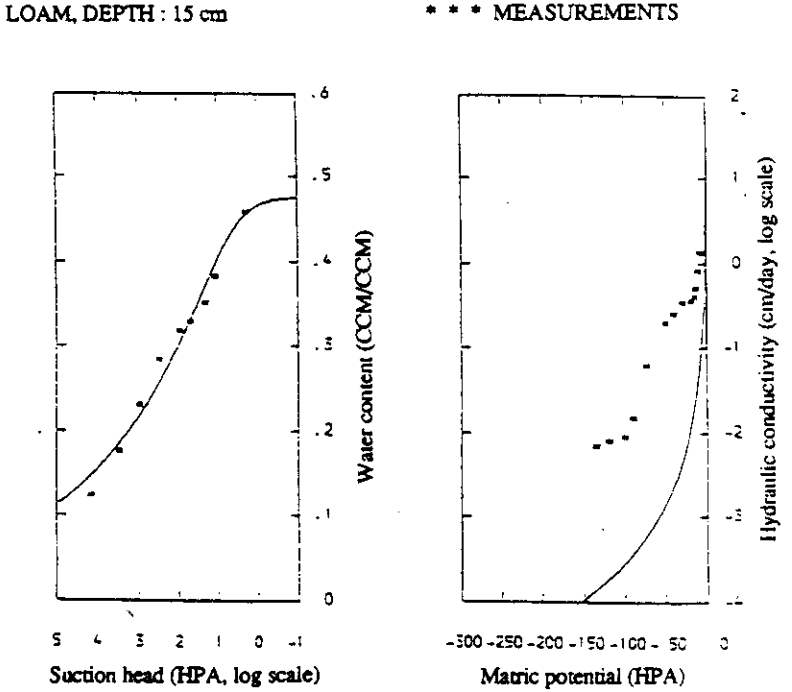

Parameter : Thetas : 47.52 Thetar : 0.01 KS : 30.00 Alpha : 0.2312 N : 1.14

Fig. 4a Prediction of the unsaturated conductivity K(h) from the soil water retention curve θ(h) for the mono-modal porous system. Directly measured data are plotted as asterisks : Ap horizon of Gleyic Luvisol.

From the SWRC we computed the relative conductivity function $K_r(h)$ according to the procedure of Mualem (1976). With the saturated hydraulic conductivity K_S as matching factor, we obtained the unsaturated conductivity function $K(h) = K_S K_r(h)$ for each sample. The resulting K(h) were compared to the directly measured data K(h) in the field by the method of Arya et al. (1975). The results of this comparative study were very unsatisfactory (see the Fig. 4a). The differences between the predicted and directly measured data of K were frequently more than one order of magnitude and the general run of the predicted and measured curves differed substantially.

When we applied a spline fit to the retention data, we confirmed that SWRC had more than one inflection point and on the derivative curve two peaks were distinct. We assumed therefore the existence of the bi-modal porous system and we split SWRC into two parts : one curve for intrapedal pores is denoted by the index i = 1, the second curve for interpedal pores is denoted by the index i = 2. The two curves compose the macroscopic SWRC on the principle of superposition. The boundary between the two porous systems, the separation pressure head h_{1f} is not simply found. We approximated it as the minimum between the two peaks on the pore size distribution curve, i.e. in the derivative curve to SWRC. The SWRC for each porous system is defined in a modified form of the van Genuchten's equation :

$$\theta_i(h_i) = \theta_{ri} + \frac{(\theta_{Si} - \theta_{ri})}{(1 + (\alpha_i h_i)^{n_i})^{m_i}} \qquad (1)$$

where θ_r is the residual soil water content, θ_S is the saturated soil water content and α, n, m are the empirical parameters determined by the fitting procedure, further on $m_i = 1 - \frac{1}{n_i}$, h is taken as positive. The relative unsaturated hydraulic conductivity is obtained from SWRC by Mualem's procedure and :

$$K_{ri}(h_i) = \frac{\left(1 - (\alpha_i h_i)^{n_i - 1}\left(1 + (\alpha_i h_i)^{n_i}\right)^{-m_i}\right)^2}{\left(1 + (\alpha_i h_i)^{n_i}\right)^{\frac{m_i}{2}}} \qquad (2)$$

where $K(h_i) = K_{ri}(h_i)K_{Si}$ and K_{S2} is the saturated conductivity of the soil as found at h = 0, while K_{S1} is the "saturated" conductivity of the first, intrapedal porous system $K(h_{1f})$ where h_{1f} the separation pressure head denotes h at the boundary between the system 1 and 2. The SWRC and K(h) of the whole soil porous system were constructed on the principle of the superposition. Both functions thus obtained have shown an improved coincidence with the measured data (Fig. 4b and Fig. 5 to 7). However, the prediction of K(h) is in some instances still unsatisfactory.

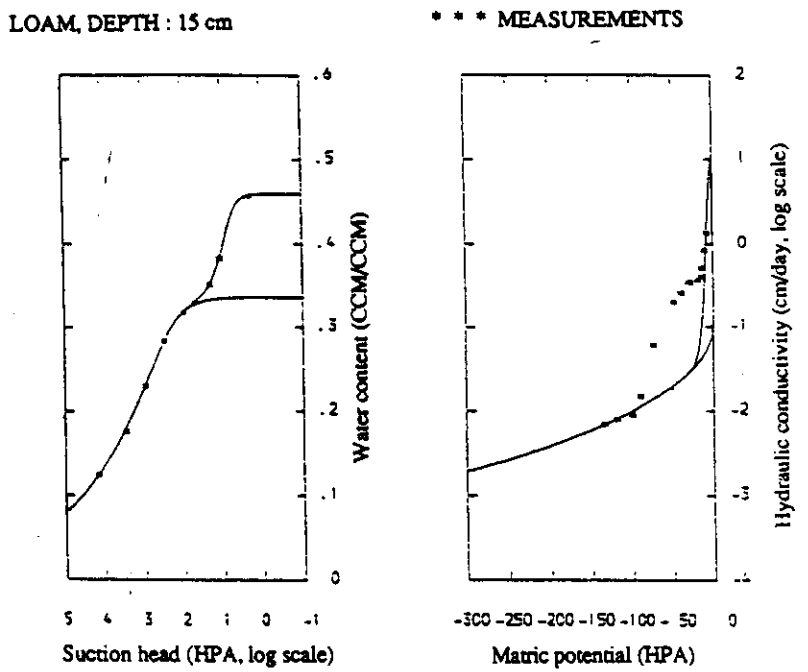

Parameter :
Pore system 1 : Thetas : 33.60 Thetar : 1.38 KS : 0.15 Alpha : 0.0039 N : 1.27
Pore system 2 : Thetas : 12.36 Thetar : 0.00 KS : 11.50 Alpha : 0.1262 N : 2.90

Fig. 4b Prediction of the unsaturated conductivity K(h) from the soil water retention curve θ(h) for the bi-modal porous system. Directly measured data are plotted as asterisks : Ap horizon of Gleyic Luvisol.

An improvement is reached when we shift the separation pressure head h_{1f} by iteration to the optimum value of predicted K(h) in relation to the measured K(h) data. The other opportunity is to split SWRC of the whole sample into 3 curves for a hypothetical 3-modal porous system in order to get the improvement in the computed K(h). However, both ameliorative procedures would be highly speculative without a direct experimental proof and without immediate applicability in the solution of the practical tasks.

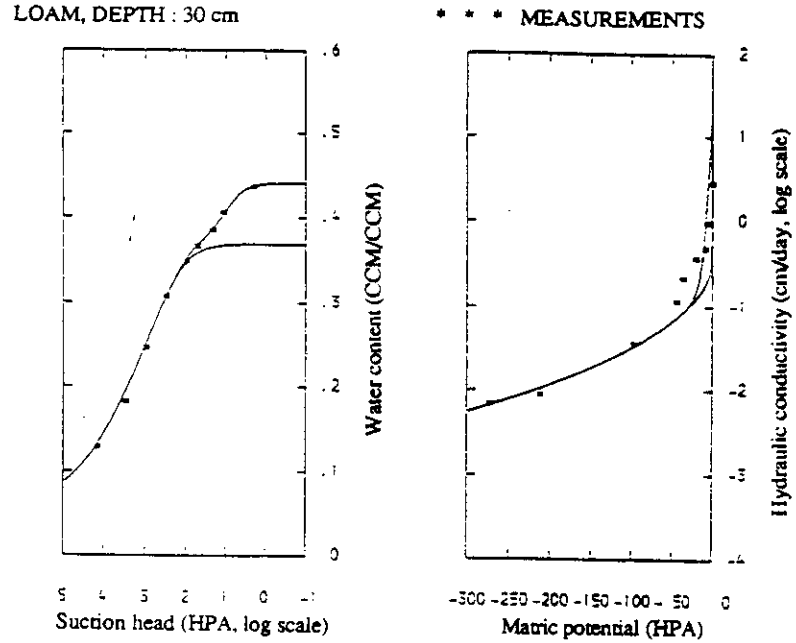

Fig. 5 Plot of θ(h) and the prediction of K(h) as in Fig. 4b. Soil from the B2t1 horizon. Bi-modal system.

For practical procedures we propose therefore to measure SWRC in small steps of h close to the saturation. When a cubic spline function is drawn, the inflection points are simply detected and the split of the SWRC can be realised. For the individual porous systems, $K_{ri}(h)$ are predicted and as matching points, we need two values of hydraulic conductivities determined in the field : K_S and K at a certain h not too far from the saturation, K_S is for system 2 and K for system 1. Let us note here the earlier proposal of Nielsen et al. (1986) on two matching points, K_S and a certain K for the realistic transformation of $K_r(h)$ to K(h).

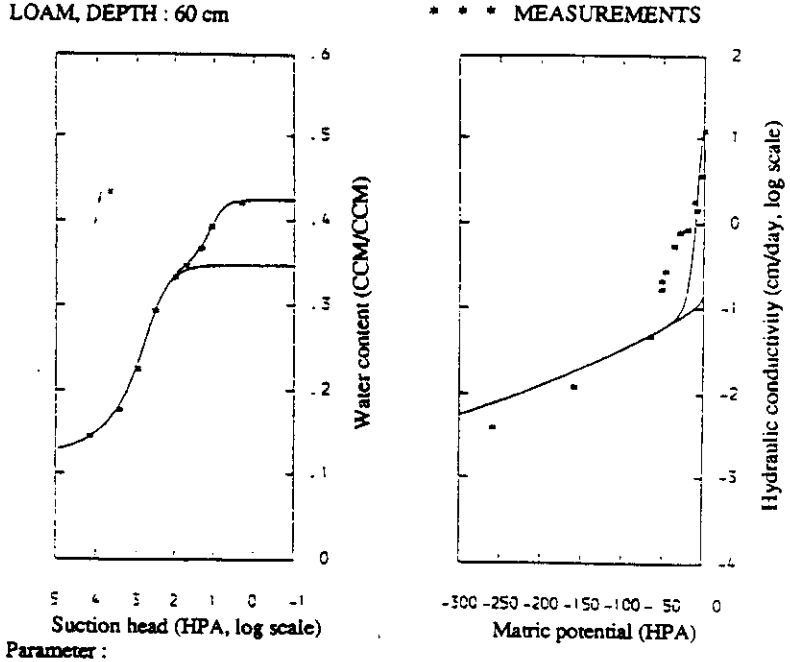

Fig. 6 Plot of θ(h) and the prediction of K(h) as in Fig. 4b. Soil from the B2t2 horizon. Bi-modal system.

In our examples in Fig. 4b and 5 to 7, the interpedal porosity plays the important role in the A and B horizons; in the C horizon is its role less significant. We have found in the literature (Othmer et al., 1991) in 11 papers of various authors that more than one inflection point was detectable in the SWRC and the bi-modal porosity could be expected in these instances. Durner (1991) quotes 14 publications where the n-modal porous systems can be deduced from the experimental SWRC. The concept of the bi-modal porosity has been recently applied in modeling the transport phenomena in soils (Diekkrüger and Sattler, 1992, Durner and Zurmühl, 1992, Rehding et al., 1992, van Genuchten, 1992).

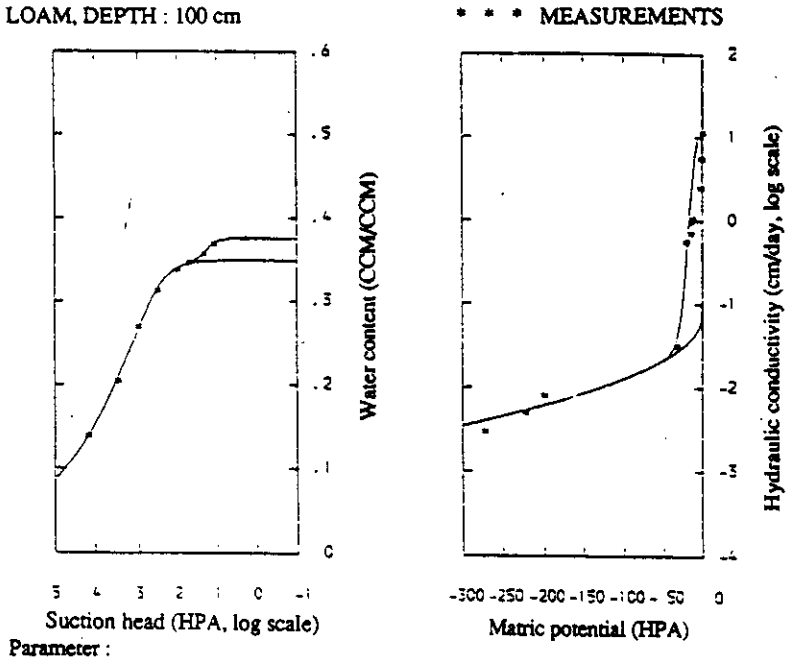

Fig. 7 Plot of θ(h) and the prediction of K(h) as in Fig. 4b. Soil from the B2g/C horizon. Bi-modal system.

3. Microscopic model studies

By the term microscopic we understand the detailed description of the porous system on the pore level. The realistic model consists of the three-dimensionally interconnected pores which form the continuous network. The behavior of water (wetting phase, wp) and of air (non-wetting phase, nwp) in the network is advantageously described by the percolation theory (Dullien, 1991). The fundamental elements of the percolation network are sites (nodes, pores) and bonds (throats). Their equivalent diameters are D^P and D^T. The network of pores and throats is regular, usually rectangular. The values of D^T are either correlated or uncorrelated to D^P. The values of D^P are randomly distributed in the infinite network. If the model consists of minimally 18 meshes in the direction of each of the three main axis, the model approaches well the behavior of the infinite model. When the model is placed in the pressure apparatus, the given pressure head h_M corresponds to the diameter D_M according to the capillary theory. The percolation theory allows us to discover the clusters of undrained pores even if their $D > D_M$. An analogical situation develops when the model is wetted and the clusters of

the closed air occur. The characteristics of the model influence the final SWRC in a typical way. For example the hysteresis is substantially influenced by the relation of D^T to D^P, the log-normal distribution of pores increases the hysteretic loop when compared to the normal distribution and the value of θ_r decreases due to the log-normal distribution. The spectrum of the pore size distribution has the influence upon the slope of SWRC, the increase of the standard deviation increases this slope. The air entry value h_A depends upon the skewness of the pore size distribution curve, etc. (Rösslerová, 1992).

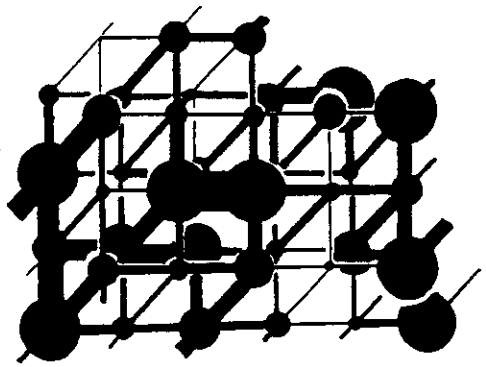

Fig. 8 Schematic presentation of the 3-d rectangular percolation network.

We have modeled the bi-modal soil porous system by the 3-d rectangular network of pores and correlated throats in the system 1 (intrapedal pores) (Fig. 8). The system 2 (interpedal pores) was modeled by the regular net of either 16 big peds or of 128 small peds. The same system of pores and throats existed between the peds as in system 1 and the only difference was in the bigger size of pores and throats in the system 2. For D1 we used the normal distribution with the mean diameter of pores $9.74\ 10^{-4}$ cm and with the standard deviation $3.8\ 10^{-4}$ cm. For D2 the distribution was normal, too, with the mean diameter of the interpedal pores $5.2\ 10^{-3}$ cm, the standard deviation was $9.6\ 10^{-4}$ cm. The size of pores inside of peds and between the peds was randomly generated.

For the network consisting of 128 peds is $\Theta_S = 0.797$ and $\Theta_r = 0.036$. For the network with 16 peds is $\Theta_S = 0.982$ and $\Theta_r = 0.161$. Since Θ is in parametric form, we get the real $\theta = \Theta P$, where P is the porosity. Θ_S denotes the saturation value at the end of the wetting process. Just for comparison, if the system was mono-modal, then for D1 we got $\Theta_S = 0.745$ and $\Theta_r = 0.019$ and for D2 mono-modal (i.e. without intrapedal pores) $\Theta_S = 0.818$ and $\Theta_r = 0.051$. In order to show the volume of isolated clusters of water or air in the drainage and wetting process, we relate D_M to the pores and throats occupied by water in Fig. 9. The bi-modal porous system is compared to the mono-modal porous system which is identical with the characteristics of intrapedal pores in the bi-modal system. We can recognize two different stages of the drainage.

In the first stage at high D_M, i.e. close to the saturation with water, the throats between the peds are readily drained while the pores between the peds are partly filled with water in clusters. The number of pores occupied by water is higher in the mono-modal model than in the bi-modal model. It means that the bi-modal system is more readily drained than the mono-modal system in the first stage.

The second stage at low D_M, i.e. far from the saturation is very different. The number of pores as well as of throats occupied by water is significantly higher in the bi-modal than in the mono-modal system. Analogical situation is for wetting, the two stages are again well recognized. When the size of peds increases, the residual content of clusters filled with water is increased, see also the value of Θ_r, but the clusters of closed air at saturation with water decreases.

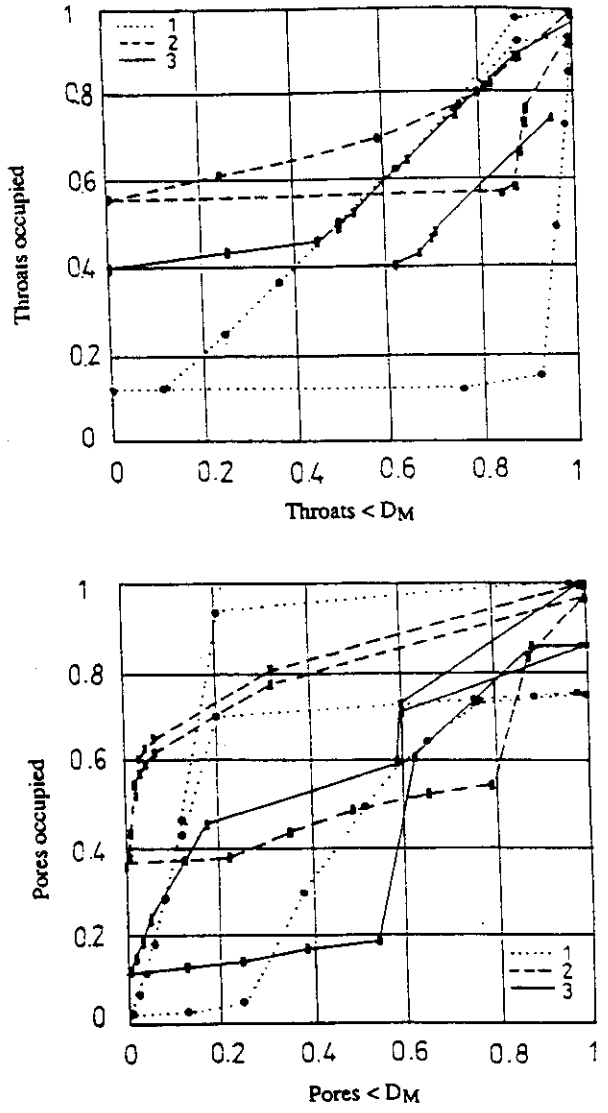

Fig. 9 The relative number of throats and pores D_M which should be drained at the given pressure. It is related to the relative number of throats and pores occupied by water : 1– mono-modal porous system, 2– bi-modal system, big peds, 3– bi-modal system, small peds.

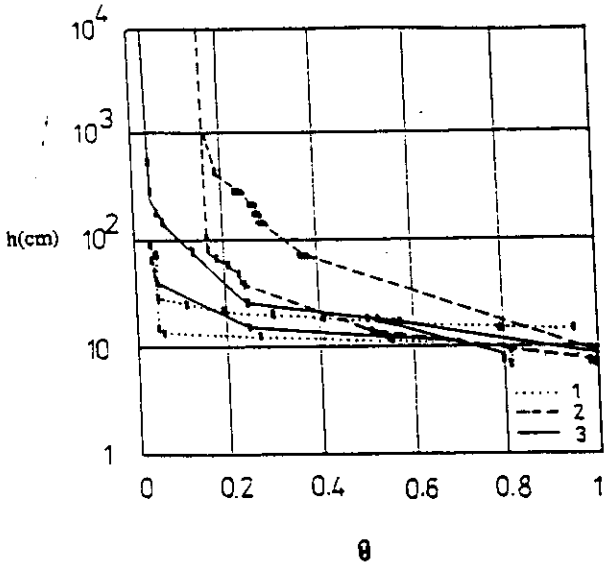

Fig. 10 Soil water retention curves with the parametric soil water content Θ : 1 – mono-modal porous system, 2 – bi-modal porous system, big peds, 3 – bi-modal porous system, small peds.

On SWRC which are plotted as parametric Θ against h (see the Fig. 10), we have detected the following tendencies due to the bi-modality of the pore size distribution :

(i) The increase of Θ_r in systems with big peds and slight decrease of Θ_r due to the small peds, when compared to the mono-modal system.
(ii) The air entry value h_A was not practically influenced by bi-modality.
(iii) The bi-modality causes an increased slope of the SWRC and the curve is just close to the shape of the SWRC of real soils. In mono-modal models the shape was close to the step-like form and thus differed from the great majority of soils.
(iv) In all studied bi-modal models we have detected 3 inflection points in SWRC. Our previous hypothesis on the existence of the bi-modality is confirmed even by the 3-d percolation models.
(v) The hysteretic loop is broader in the bi-modal systems.

When SWRC are described by the van Genuchten's equation, then the introduction of the bi-modal system is reflected by the decrease of both parameters, n and α. The increase of the standard deviation of pore size distribution decreases the value of the parameter n.

This first study is still far from the development of methods for the physical interpretation of parameters in equations describing SWRC. It shows only the possibilities of the physical modeling of SWRC when the models are close to the real soil porous systems.

4. A note on the stability of the soil porous system

In all our studies on the non-steady transports in unsaturated soils, the concept of the rigid and stable arrangement of the soil porous system is accepted. We are not speaking on the large time alteration of the soil porous system due to the activity of the soil edaphon, but on the possible changes in short time during the wetting or drying process in the soil. If we define three or four domains of volumetric changes in clay soils (Haines, 1923, Yule and Ritchie, 1980), we have to admit that the shrinkage and swelling may result in the transformation of the soil porous system and that the macroscopic change is accompanied by the change on the pore scale.

Schweikle (1982) brought the evidence on the change of the porous system in clay aggregates. He published the summation curves of pores measured by the mercury porometry. We have used his data for the derivation of the pore size distribution in the wet soil, h = 0 and in the dry soil, h = –1.5 MPa (Fig. 11).

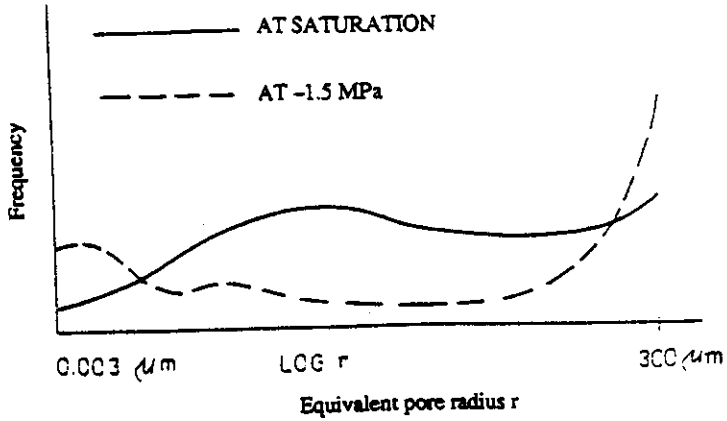

Fig. 11 Pore size distribution in clay aggregates at the water saturation and at the wilting point (i.e. at the pressure head –1.5 MPa) according to the data of Schweikle (1982).

The interpretation is in the traditional way when the full access of all pores to sinks and sources exist. The difference is striking. When the soil is saturated with water, the pore size distribution is near to the mono-modal type with slightly higher frequency of coarse pores and with low content of ultrafine pores. The mean equivalent radius is of

the order of units µm, i.e. at the medium pore size. When the soil was drained up to h = –1.5 MPa, the pore size distribution changed substantially. The frequency of the medium pores is now at minimum, the shrinkage reduced this category of pores and the coarse pores gained a very high frequency. Great portion of medium pores was transformed into coarse pores. A smaller portion of medium pores was compressed and transformed to fine and ultrafine pores, where the bi-modal pore size distribution developed. However, from this scarce experimental evidence we can not conclude if the transformation of the pore size distribution due to the change in soil water content is significant for majority of soils.

Acknowledgements

We are pleased to acknowledge Dr. B. Diekkrüger from the Technical University in Braunschweig for his advices and cooperation on the theory of the bi-modal porosity. The financial support of SCP 179 by the German Research Foundation (DFG) is acknowledged with thanks, too.

References

- Arya, L.M.D., D.A. Farell and G.R. Blake, 1975. A field study of soil water depletion patterns in presence of growing soybean root : I. Determination of hydraulic properties of the soil. Soil Sci. Soc. Am. Proc. 39 : 424–436.
- Bouma, J., 1991. Influence of soil macroporosity on environmental quality. Advances in Agronomy, 46 : 1–37.
- Brewer, R., 1964. Fabric and Mineral Analysis of Soils. John Wiley and Sons, New York.
- Diekkrüger, B. and A. Sattler, 1992. Analysis of preferential flow in soils. Poster at Intern. Congr. Agro-Ecosystem Modelling, 5–9 Oct. 1992, TU Braunschweig.
- Dullien, F.A.L., 1991. Characterization of porous media – Pore level. Transport in Porous Media 6 : 581–606.
- Durner, W., 1991. Vorhersage der hydraulischen Leitfähigkeiten strukturierter Böden. Doktor-Dissertation, Universität Bayreuth.
- Durner, W. and T. Zurmühl, 1992. Numerical modeling of water and tracer transport in biporous soil. Report at Intern. Congr. Agro-Ecosystem Modelling, 5–9 Oct. 1992, TU Braunschweig.
- Germann, P.F. and K. Beven, 1985. Kinematic wave approximation to infiltration into soils with sorbing macropores. Water Res. Res. 21: 990–996.
- Haines, W.B., 1923. The volume changes associated with variations of water content in soil. J. Agric. Sci. 13 : 293–310.
- Mualem, Y., 1976. A new model for predicting the hydraulic conductivity of unsaturated porous media, Water Res. Res. 12 : 513–522.
- Nielsen, D.R., M.T. van Genuchten and J.W. Biggar, 1986. Water flow and solute transport processes in the unsaturated zone. Water Res. Res. 22 : 98S–108S.
- Othmer, H., B. Diekkrüger and M. Kutílek, 1991. Bimodal porosity and unsaturated hydraulic conductivity. Soil Sci. 152 : 139–150.

- Rehding, Ch. W. Durner and R. Herrmann, 1992. Field scale monitoring of preferential transport of bromide through unsaturated soil. Poster at Intern. Congr. Agro-Ecosystem Modelling, 5–9 Oct. 1992, TU Braunschweig.
- Rösslerová, R., 1992. Percolation models : Application for the interpretation of soil water retention curves (in Czech). PhD Thesis, Czech Technical University, Prague.
- Schweikle, V., 1982. Gefügeeigenschaften von Tonböden. Verlag Eugen Ulmer, Stuttgart.
- Van Genuchten, M.T., 1980. A closed form equation for predicting the hydraulic conductivity of unsaturated soils. Soil Sci. Soc. Am. J. 44 : 892–898.
- Van Genuchten, M.T., 1992. A dual porosity approach for modelling water and solute movement. Report at Colloquium Porous of Fractured Unsaturated Media : Transport and Behavior, Monte Verità, 5 – 9 Oct. 1992.
- Yule, D.F. and J.T. Ritchie, 1980. Soil shrinkage relationships of Texas vertisols : I. Small cores. Soil Sci. Soc. Am. J. 44 : 1285–1291.

Address of the authors

M. Kutílek and R. Rösslerová, Czech Technical University, Faculty of Civil Engineering, K143, Thakurova 7, 16629, Prague 6, Czechoslovakia.

H. Othmer, Technical University, Braunschweig, now : Schunterstrasse 55a, 3300 Braunschweig, Germany.